Durham University

Evaluation of metal stress on the composition of Ulva spp. biomass-for-biofuel.

Ana Cristina Reyes Monarrez

Submitted for the qualification of Master of Science (MSc)

Department of Biosciences, Durham University

October 2019

Abstract

This work assesses the suitability of *Ulva spp*. as a biofuel crop. Since earlier research has demonstrated the relation between metal handling mechanisms and diverse changes in lipid content, we attempt to elucidate how lipids are stored within the cell by carrying out genetic expression studies and fluorescence microscopy. So far, *Ulva* thalli has been exposed to lead (Pb) and a combination of this metal with Buthionine sulfoximine (BSO), an inhibitor of glutathione (GSH) synthesis, with the aim of comprehend the effects of lead on lipid content as well as the way they organise in the form of lipid droplets (LD). BSO was added to determine whether this caused changes in *Ulva*'s metal handling mechanisms. Results from fluorescence microscopy and genetic expression studies have showed that even though lead does not increase the amount of lipid in the cell, it causes changes in lipids localisation and dynamics. Moreover, it was observed that samples treated with BSO present fewer and smaller lipid droplets. To clarify BSO's role in lipid droplet formation and get a better understanding of the pathways involved in heavy metal handling, further transcriptome and metabolic studies need to be performed. The elucidation of these mechanisms will ease biofuel production from macroalgal species like *Ulva spp*. This knowledge can be applied in countries like Mexico since *Ulva* and similar seaweed can be harvested in coastal areas around the world as a biofuel crop.

Table of Contents

List of figures

List of tables

Acknowledgements

First of all, I would like to express my gratitude to Dr John Bothwell, his guidance, help and support have definitely been essential for this project to work. I will always thank him for encouraging me to experiment all the aspects of scientific research and not only the lab/office bits. Thanks, Doc! Thanks to my lab mates and the team from Lab 5 in the department of Biosciences, for your contribution to this achievement.

My studies in Durham University would not have been possible without the help of the CONACYT-SENER sectorial fund, who has provided the scholarship for my masters. Thanks to these two institutions I was able to come to England and learn as much as I could to try to make of my country a better place. This opportunity is invaluable, and I will thank for it the rest of my life. I am truly a proud Mexican who had the chance to go out and give her best for Mexico.

I also desire to express my sincere and total gratitude to Prof Teresa Alonso, whose guidance, help and support have been crucial, thanks for teaching me to think out of the box and be such a good model of loyalty to our country. I hope to follow that path and serve to Mexico in such a devoted way.

To Durham University and the Biosciences Department for being so welcoming and always willing to help during this journey. To Fiona O'Carroll, Evelyn Tehrani, the International Office and all the team who made the Pre-sessional at Mexico possible in 2017. To Christine Richardson, Buddhika Mendis and Diego Perera, thanks for helping and assisting me while running my experiments and the possibility to work in more than one department. To Dr Moenne´s team in the University of Santiago de Chile (USACH), who have helped this project to look as promising and complete as it is. Their work has been very important to define the track we followed.

Last but not least, I want to thank Dr Jesus Gabriel Rangel Peraza for introducing me to the world of research and teaching me how to survive. Thanks to Dr Rangel's team at Instituto Tecnologico de Culiacan for all your support and company throughout the process. To my parents and sister, who have been incredibly supportive and encouraging for this.

1 Introduction.

1.1 The necessity of alternative energy sources.

Energy is one of humanity's most important requirements. However, the demand for many fuel types is increasingly higher than the capacity of the planet to supply them, and the likelihood of an energy crisis increases yearly (Baños et al., 2011).

The bulk of global energy is currently generated from non-renewable (fossil) fuels, but there is only a limited reserve of such fuels and this reserve is rapidly being depleted (Abomohra, El-Naggar and Baeshen, 2018). Furthermore, the intensive use of these fuels has increased our Greenhouse gas (GHG) emissions in the last decades, causing a major impact in climate change and global warming. About 78% of GHG emissions are caused by fossil fuels combustion (IPCC, 2014).

Diverse alternatives have been proposed to mitigate the quick fuel depletion as well as the GHG emissions. Wind, solar, geothermal, marine and biomass energy have been proposed and studied to diverse extents (Lund, 2007). Nonetheless, it was estimated that renewable sources only supplied 12.9% of primary energy production in 2008 (Moomaw et al., 2011). Even though renewable energy contributions are still relatively small, their use is increasing. In fact, in 2006, the European Renewable Energy Council (EREC) estimated that renewable sources of energy would provide half of the total energy requirements by 2040 (Demirbas, 2009a).

According to the IPCC's Report on Renewable Energy Sources and Climate Change Mitigation (Moomaw et al., 2011), the International Energy Agency (IEA) reported biomass as the major renewable energy source used in 2008. Many renewable forms of biomass can be converted into a variety of replacement fuels, such as biogas, bioethanol, or biodiesel. Of these, liquid biofuels such as bioethanol and biodiesel are particularly promising since they possess similar properties to current liquid combustible fuels (Agarwal, 2007), which are much in demand as replacement transport fuels. Since they are produced from photosynthetic sources, biofuel use is carbon neutral, reducing contaminants and GHG emissions (El Maghraby and Fakhry, 2015). Moreover, the potential of a whole new biomass industry might be beneficial for developing countries, reducing external dependence, and bringing an economic boost (Saga et al., 2008; Demirbas, 2009b).

Biodiesel is particularly interesting since it can substitute traditional diesel without requiring any engine adaptation (Demirbas, 2009a). Besides its limited reserves, petrochemical diesel contains a high proportion of sulfur and particulate material. It has also been reported to produce a third of the GHG emissions from transport activities (Nas and Berktay, 2007). In contrast, biodiesel, which consists of fatty acid methyl or ethyl esters obtained from vegetable oils or animal fats via transesterification (Vicente et al., 2004), presents lower particulate material and emits less hydrocarbons and carbon monoxide (EPA, 2002).

1.2 Algae as a biomass source.

Strong feedstock prospects to provide biofuels are crops that grow rapidly and for which the farming infrastructure already exists, such as corn, sugarcane or high lipid content species like soybean or sunflower (Abomohra, El-Naggar and Baeshen, 2018; Wei, Quarterman and Jin, 2013). Unfortunately, all these species are already valuable food crops and their use as biofuel raises many ethical issues (John et al., 2011). To satisfy current fuel requirements, food supply may be threatened because of insufficient arable land and water (El Maghraby and Fakhry, 2015), which is an especial problem in developing countries such as India, Indonesia, Brazil, or Mexico.

For these reasons, many other possible biomass sources have been considered in recent years. Some authors have classified biofuels by ‘generations’; each biofuel generation is characterised by its biomass source and their production technologies (Table 1).

Table 1 Classification of biofuels (Demirbas, 2009c).

Generation	Feedstock	Examples
First	Sugar, starch, vegetable oils or animal fats (edible).	Bioethanol, biogas, vegetable oil, biodiesel, biosyngas.
Second	Non-food crops, wheat straw, corn, wood, solid waste (bagasse), energy crops (lignocellulosic).	Bioalcohols, bio-oil, bio-DMF, Biohydrogen, bio-Fisher-Tropsch diesel, wood diesel.
Third	**Algae**, gene modified crops	Vegetable oil, **biodiesel**, bioethanol.
Fourth	Vegetable oil, biodiesel.	Biogasoline.

As a first response to the issues raised by first generation biofuels, second generation feedstocks were proposed. These new materials were considered a convenient option since they are mostly waste materials or non- edible crops (Demirbas, 2009b). Despite their advantages, second generation feedstocks are not as well-known as first-generation ones, making necessary further research on harvesting and biorefinery techniques (Naik, Goud, Rout & Dalai, 2010). For example, these materials contain lignin, an amorphous carbohydrate which is highly difficult to degrade, making it harder to extract and process biomass components (Sánchez, 2009; Chávez-Sifontes & Domine, 2013; Demirbas, 2009c).

Macroalgae and microalgae are prominent candidates to substitute lignocellulosic materials. Algae present diverse advantages over land plants such as a faster growth rate, greater potential to reduce CO_2 pollution, lack of competition for arable land and freshwater, and easier depolymerisation since they contain less or no lignin (Abomohra, El-Naggar and Baeshen, 2018). Thus, algae can grow in a broad variety of conditions, including stressful environments, making the possibilities of novel processes and techniques wider (Goh & Lee, 2010). These advantages mean that algae are considered a “low input, high yield” crop

(Sheehan, et al., 1998). However, since algae are not a common crop, the current information about them is limited. It remains a challenge to harvest seaweeds at consistent high yields (Wei, Quarterman and Jin, 2013), making it critical to improve our understanding of their composition (Michalak, 2018).

1.2.1 Potential of Ulva as biomass source.

Among macroalgae, the attention of researchers has been drawn to the *Ulva* genus mainly because of its high growth rate as well as its natural capability to grow in a broad range of environmental conditions which allows 'bloom' growth. It has been considered for several stress studies and for complex metabolic mechanistic research (Kumari, Kumar, Reddy & Jha, 2013; Mellado, Contreras, González, Dennett & Moenne, 2012).

Ulva also has potential as model organism due to its high tractability for genetic studies and can be easily found in many places around the world, making every technology developed from its harvesting accessible to everyone (De Clerck et al., 2018). Its high growth rate as well as its resistance to stress makes *Ulva* species promising candidates for bioremediation processes (Bolton, Cyrus, Brand, Joubert & Macey, 2016). Understanding these mechanisms is crucial to start taking advantage of *Ulva* and other algal species.

1.3 The composition of biomass depends on growth conditions

Composition is a key factor for biofuel crops. For instance, bioethanol is better produced from carbohydrate rich sources, while biodiesel needs to be made from lipid rich cells (Michalak, 2018). Biodiesel is generally considered to be the most promising main combustible alternative given the benefits it carries such as renewability, non-toxicity, its biodegradability, and compatibility with current internal combustion engines (El Maghraby and Fakhry, 2015).

One of the most proposed biodiesel feedstocks are the microalgae, because of their high lipid contents, which can go up to 75% in the microalga *Botryococcus braunii* (Michalak, 2018; Chisti, 2007). Although the larger macroalgae are faster and cheaper to harvest due to their size and plant-like structure (Abomohra, El-Naggar and Baeshen, 2018), they are not generally considered a good choice over microalgae because of their low lipid contents, which are typically lower than 5% when contents of 10% or higher are recommended for biodiesel making, although some seaweed species can go higher (Gosch et al., 2012). A study carried out

in Spain with several macroalgal species like *Sargassum muticum, Ulva rigida,* and *Enteromorpha intestinalis* showed that, given their low oil content, large amounts of seaweed are required to get viable biodiesel yields (Maceiras, Rodríguez, Cancela, Urréjola & Sánchez, 2011). Therefore, finding a way to increase macroalgal oil content is essential to make it a suitable biofuel crop.

Importantly, algal biomass compositions are often highly dependent on growth conditions and several studies have shown algal compositional changes in response to environmental stress. For example, increases of lipid content have been reported because of nitrogen starvation, changes in temperature, salinity, and heavy metals (Adams, et al., 2013; Upchurch, 2008). Taking advantage of this, some studies have tried to change lipid levels via diverse stress types (Pyc et al., 2017; Salama et al., 2013; James et al., 2011). Mohy El-Din (2017) reported that chemical stress augments lipid content in marine *Pterocladia capillacea*, *Sargassum hornschuchii* and *Ulva lactuca.* Their study exposed algae to pharmaceuticals and endocrine-disrupting compounds and assessing their effects on lipid content. Mohy El-Din concludes that ramphenicol, acetyl salicylic acid, clofibric acid and nonylphenol increased fatty acid (FA) contents in algal cells. Furthermore, Yeh and Chan (2011), Sun et al. (2014) and Fakhry and El Maghraby (2015) also claim that nitrogen starvation increases lipid levels.

Accordingly, my project will use metal stress to elicit changes in algal composition. Heavy metal pollutants may modify metabolic pathways because plants are capable of bioaccumulating them (Emamverdian et al., 2015). In addition, this bioaccumulation has the additional benefit of being a potential bioremediation process, as mentioned above. It has been reported that aquatic plants such as *Eichornia crassipes* (water hyacinth) can remove heavy metals from water bodies due to their bioaccumulation capacity (Atehortua & Gartner, 2013, Agunbiade, Olu-Owolabi, & Adebowale, 2009, Míguez, et al., 2014). Therefore, harvesting macroalgae might also help to clean polluted marine water.

1.4 Greater understanding of algal stress responses will allow biomass manipulation

It is well known that changes in metabolism follow exposure to stress. A major metabolic change that often accompanies stresses is a shift from carbohydrate metabolism to lipid metabolism. For instance, drought stress inhibits photosynthesis and deactivates invertases (INVs) in maize (*Zea mays*), which decreases starch biosynthesis (Ruan et al., 2010). Low sugar

levels cause the breakdown of storage starch and lipids in higher plants (Thakur, Kumar, Malik, Berger, & Nayyar, 2010). Temperature changes can also affect the biophysical properties of cellular compounds (e.g. their rheology) and reduce the activity of various enzymes, modifying metabolic pathways (Mathur, Agrawal and Jajoo, 2014). This suggests that lipid levels might vary depending on stress. However, not every kind of stress can produce the type of lipids that biodiesel production requires (Goold et al., 2016).

Besides growth rate, availability and harvesting costs, the lipid profile is also an important aspect of determining whether a species is suitable as a biodiesel feedstock. Triacylglycerols (TAGs) are compounds of interest since they are important sources of fatty acids, and they lack phosphorus, sulfur and nitrogen, which can interfere with biofuel yields (Michalak, 2018, Suutari et al., 2014). Moreover, high amounts of saturated fatty acids are required to get satisfactory generation of biodiesel (Gosch et al., 2012). Hence, a deeper knowledge of lipid biosynthesis, as well as the way cells store these compounds, is crucial.

Neutral lipids, Triacylglycerols (TAGs), Diacylglycerols (DAGs), Sterol esters (SEs), polyisoprenes, *et cetera*, are stored in structures called Lipid Droplets (LDs), which are present in every kind of organism and are a significant factor to consider for biodiesel and other lipophilic bioproducts (Pyc et al., 2017). Lipid droplets (Figure 1) are typically composed of a core of TAGs and SEs, surrounded by a monolayer made mainly of phospholipids and some proteins (Guo et al., 2009). It has been suggested that these structures perform a significant role in cell biology beyond energy storage (Welte, 2015; Fujimoto & Parton, 2011). Despite their presence in all organisms and their well conserved pathways, lipid droplet composition and biogenesis vary appreciably from one species to another (Pyc et al., 2017, Guo et al., 2009).

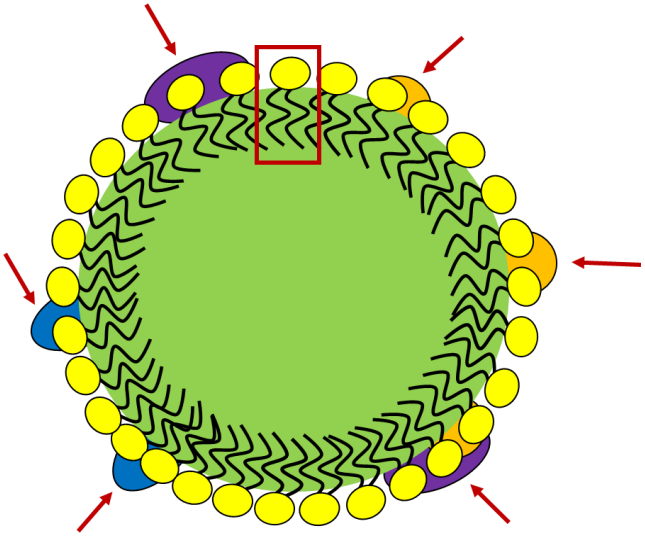

Figure 1 Lipid droplet
The picture above shows a representation of the main parts of a lipid droplet such as the neutral lipid core (green), the phospholipid monolayer (highlighted in square) and some membrane proteins (arrows).

Lipid droplets have been widely studied in mammals, insects, and yeast, but their processes and pathways are less well understood in plants. Studies in these organisms and the green microalga *Chlamydomonas reinhardtii* have made possible a general understanding of lipid droplet biogenesis (Pyc et al., 2017, Guo et al., 2009, Li-Beisson, 2018) as figures 2-5 show:

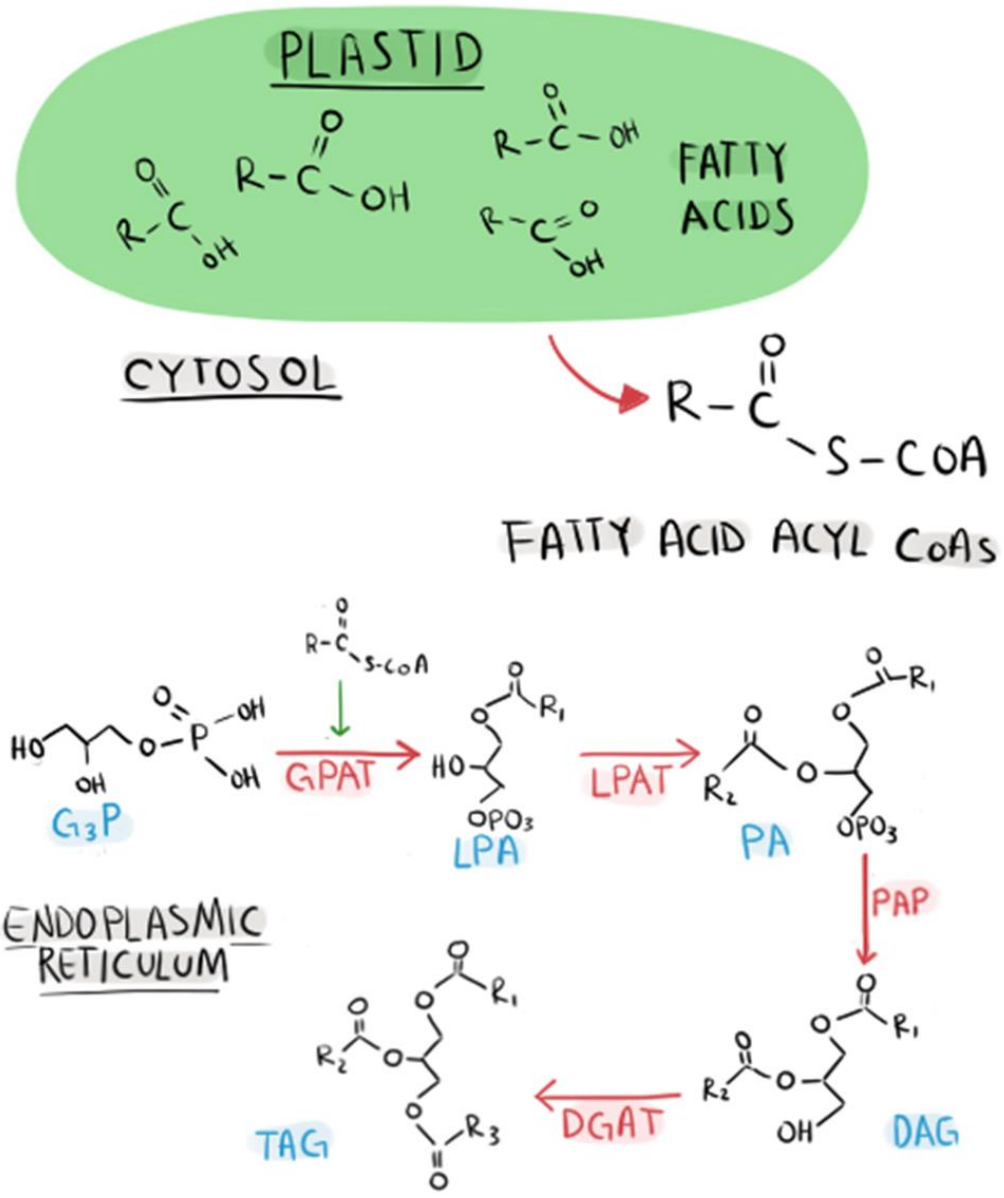

Figure 2 Pathways for Triacylglycerol biosynthesis in Chlamydomonas reinhardtii.
Abbreviations: DAG, diacylglycerol; GPAT, glycerol-3-phosphate acyltransferase; G3P, glycerol-3-phosphate; LPAT, lysophosphatidic acid acyltransferase; LPA, lysophosphatidic acid; PA, phosphatidic acid; PAP, phosphatidic acid phosphatase; TAG, triacylglycerol.

1. Fatty acids and sterols are synthesised *de novo* or obtained extracellularly.
2. Fatty acids and sterols are transformed into TAGs or sterol esters respectively in the endoplasmic reticulum (ER).
3. Neutral lipids are synthesised in the endoplasmic reticulum by Diacylglycerol O-acetyltransferase (DGAT), Glycerol-3-phosphate acyltransferase (GPAT) and other ER enzymes.
4. Neutral lipids accumulate between the two leaflets of the endoplasmic reticulum membrane and form a 'lens-like' structure.
5. Fat storage-inducing transmembrane protein (FIT2), which not present in plants, or any other endoplasmic reticulum's membrane protein brings TAGs to make the 'lipid bubble' grow and bud from the ER.
6. Lipin family proteins are incorporated to the phospholipid monolayer for future DAGs synthesis.

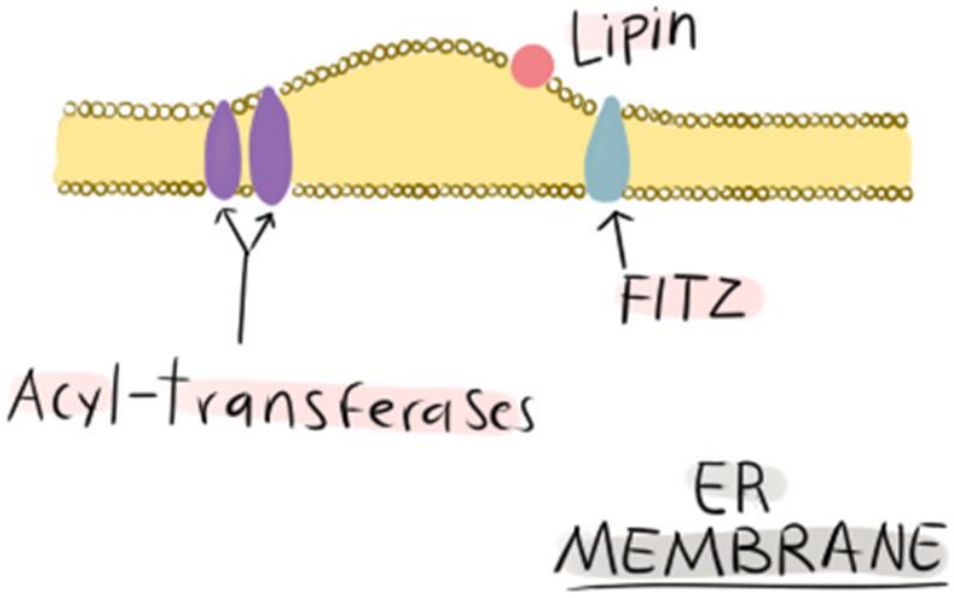

Figure 3 Lipid droplet formation a).
Steps 4, 5 and 6 of. Neutral lipids are incorporated to the 'lens structure' via membrane proteins' action. Lipin is added to the lipid droplet's surface for future lipid synthesis.

7. SEIPIN (a lipodystrophy protein) incorporates new lipids and proteins to lipid droplets and transforms them into mature structures.
8. Choline-phosphate cytidylyltransferase 1 (CCT1) is recruited to coordinate phospholipid synthesis in the expanding lipid droplet's monolayer.

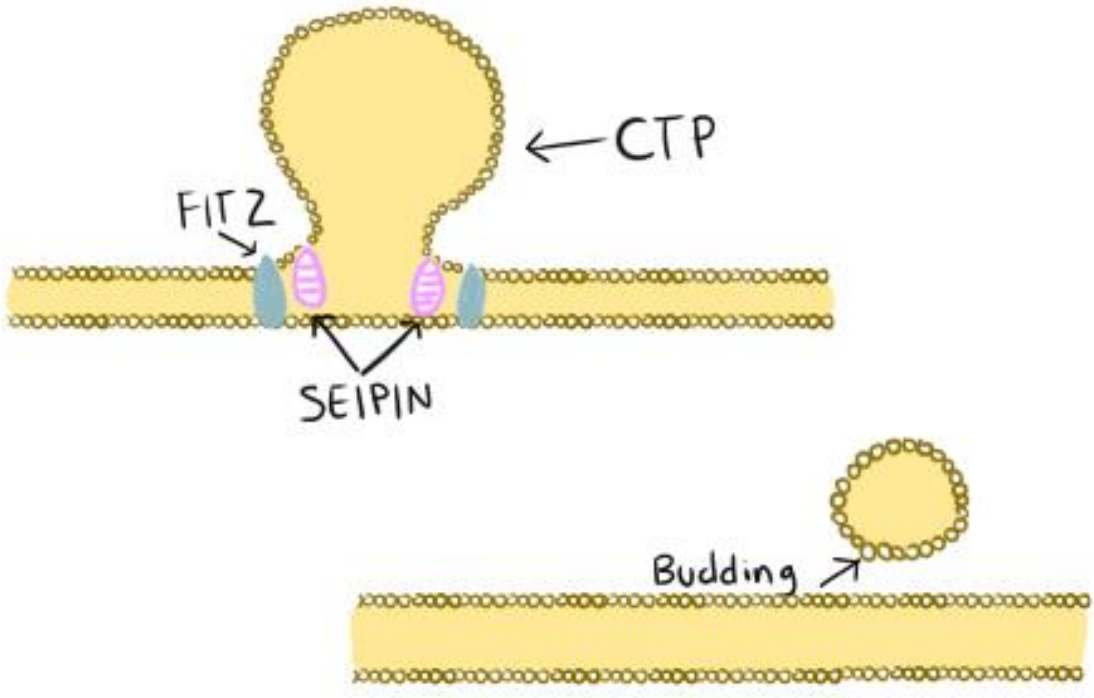

Figure 4 Lipid droplet formation b)

Steps 7 and 8. SEIPIN transforms the lipid droplet into a mature structure by adding more lipids and proteins. CTP regulates this action.

9. During their life cycles, lipid droplets can stay connected to ER and grow there via SEIPIN action or expand in the cytoplasm by fusion or lipid transfer.

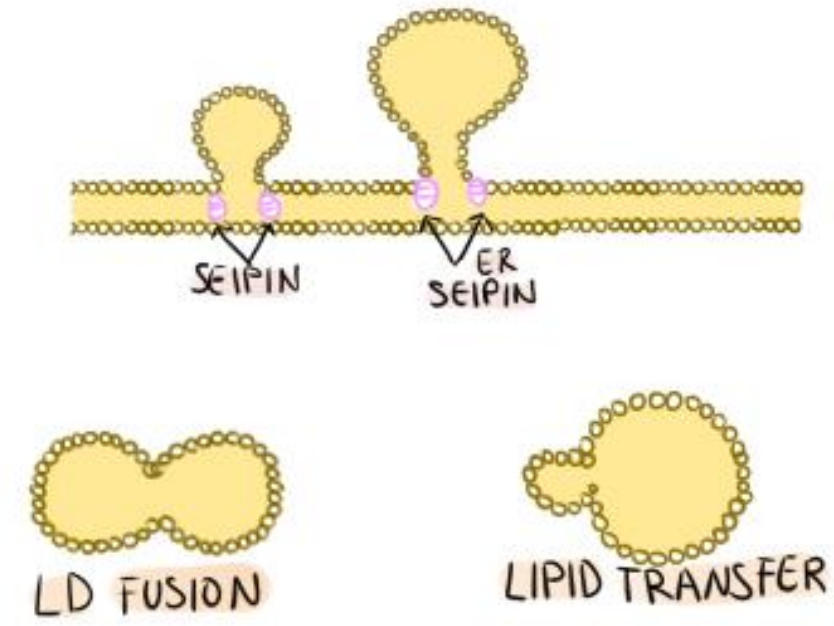

Figure 5 Life cycle of a lipid droplet.
A mature lipid droplet can stay attached to the endoplasmic reticulum for energy storage or bud from the ER membrane to stay in the cytosol.

Since most steps in the lipid droplet biogenesis pathway are widely conserved, bioinformatic studies have been a useful tool to start clarifying lipid droplet processes in plants. Homology searches in mammals and yeasts have been one of the most helpful ways to elucidate lipid droplet mechanisms and identify the roles of every component. For instance, it has been discovered that the perilipin family, which stabilise the lipid droplet structure, is not present in plants. Instead, this job is performed by oleosins in vegetal cells (Guo et al., 2009). In the same way, several accessory proteins have been identified. Small rubber particle proteins (SRPPs) were reported as the most abundant protein in avocado lipid droplets (Pyc et al., 2017). SRPP-like proteins were also found in Arabidopsis; however, since rubber is not present in these cells, this protein was named Lipid Droplet Associated Protein (LDAP) (Pyc et al., 2017). LDAP is found at the surface of LDs and modulates their proper compartmentalisation; this protein is specific to plants and algae. Moreover, studies have highlighted that LDAPs perform an important role in temperature and drought stress (Pyc et al., 2017). Salt stress (Kim et al., 2016) as well as phosphorous and nitrogen starvation (Iwai, Ikeda, Shimojima & Ohta, 2014;

Liu, Wang & Zhou, 2008) have been proven to cause an increase in lipid droplets in *Chlorella vulgaris* and *C. reinhardtii*.

1.5 Lipid droplets in macroalgae

As previously mentioned, macroalgae do not usually contain enough lipid to be used as biodiesel feedstock. Therefore, finding a way to increase lipid levels has been proposed as a promising step towards greener energy. One way to achieve this would be to modify gene expression to augment lipid droplet formation (Pyc et al., 2017). In addition, it has been observed that different types of stress produce different types of lipid droplets. Given the high levels of heavy metal present in polluted marine ecosystems, metal stress will be particularly studied in this research as a tool for increasing lipid content.

In addition, ectopic expression of known lipid droplet proteins has been suggested as an effective strategy to trigger lipid droplet formation. Cai et al., (2017) have successfully expressed mouse FIT2 protein in *Nicotiana tabacum*, *Nicotiana benthamiana* and *Arabidopsis thaliana*, getting an elevation of lipid droplets in *N. tabacum* suspension-cultured cells, *N. benthamiana* leaves and *A. thaliana* plants. It is possible to assume that most of the cell's carbon supply goes to fatty acid synthesis, direct those fatty acid to TAG production, stimulate lipid droplet formation and keep them stable by lipid droplet related gene overexpression in what are called "push, pull and protect" strategies. Cai achieved this by overexpressing LEAFY COTYLEDON2 (LEC2) to 'push' carbon to fatty acids synthesis, DGAT2 to 'pull' fatty acids to become TAGs and introducing FIT2 to stimulate lipid droplet formation in tobacco leaves. Hence, this might be a convenient strategy once lipid droplet proteins and their expression are better known. To measure the effectiveness of this treatments in macroalgae, lipid droplets need to be observed and analysed.

The most immediate way to measure lipid droplet shape, number and size is microscopic imaging. Electron microscopy and Fluorescence microscopy are two possible approaches, but there are several points that must be considered. On the one hand, electron microscopy makes it impossible to observe the lipid droplet's limiting membrane, smaller lipid droplets are much harder to identify due to their low density and, given their diverse composition, staining agents may not cover all lipid droplets to the same level. In addition, common sample preparation techniques tend to destroy lipid droplet structure (Ohsaki, Suzuki and Fujimoto, 2014). On the

other hand, even though fluorescence microscopy makes smaller lipid droplets easier to observe, lipophilic dyes may cause some problems. For instance, they may modulate lipid droplet activity or produce uneven labelling (Ohsaki, Suzuki and Fujimoto, 2014). Despite this, fluorescence microscopy provides better contrast to observe lipid droplets of all sizes besides its quicker and more convenient results. Therefore, it will be the technique used for this research.

Even though lipid droplets have been observed in *Ulva* cells, a broader and deeper study on their formation pathways and their dynamics is still needed. As mentioned above, TAG synthesis is well studied in microalgal species like *C. reinhardtii* as well as in several land plants. To increase the number of lipid droplets in *Ulva* cells and, consequently, to improve lipid extraction yields a better understanding of *Ulva*'s metabolic pathways is required.

2 Hypotheses and aims.

A variety of studies have shown that green seaweeds of the *Ulva* genus have high total lipid contents (El Maghraby and Fakhry, 2015), and this species is being developed in our laboratory as a green algal model species.

2.1 Hypotheses

To start this research the next hypotheses were raised:

- Metal stress increases lipid content in *Ulva* cells.
- Lipid droplets expand and multiply after metal exposure.

Understanding how metals trigger lipid changes, we may be able to trigger these lipid increases independently and increase lipid content in *Ulva* on demand, making it more amenable for biodiesel production.

2.2 Aims

To test my hypotheses, the following activities (objectives) were carried out:

- General literature review about lipid droplets.
- Explain lipid droplet formation processes in *Ulva* by identifying ubiquitous metabolic pathways.
- Identify enzymes involved in these pathways.
- Search the corresponding sequences (protein or nucleotide) for lipid droplet proteins in known genomes such as *C. reinhardtii* and *Arabidopsis thaliana*.
- Blast those sequences against the *Ulva mutabilis* genome to see which of them (lipid droplet proteins) are present.
- Share the list with our collaborators in the University of Santiago de Chile (USACH) who have carried out the differential expression studies.
- Fluorescence microscopy to observe lipid droplet dynamics.
- X-Ray diffraction analysis to determine heavy metal localisation in *Ulva* cells treated with lead.

The data retrieved from this project will allow us to develop two research directions. First, it will inform our understanding of how the composition of cultivated macroalgae is affected by environmental stress. This will help to determine the optimal conditions to get improved algal

feedstock. Second, by using metals as a tool to elicit lipid droplet responses, we can probe the mechanisms of lipid metabolism and build on these to think about how we might transform macroalgae to improve lipid yields.

3 Materials and methods

3.1 Chemicals and solutions

3.1.1 Artificial seawater (ASW)

The Table 2 shows the formulation for the preparation of 1L of ASW:

Table 2 ASW preparation

Chemical (Sigma)	Amount (g)
Seasalts	35
Sodium nitrate	0.07
β-glycerophosphate disodium salt hydrate	0.01

All the salts were dissolved in Ultrapure water (UPW).

3.1.2 Metal stocks

Table 3 shows the amounts of chemical used to get 1 ml of each metal stock:

Table 3 Metal stocks

Chemical (Sigma)	Amount (mg)	Concentration (mM)
Lead acetate trihydrate	3.79	10
Copper sulfate pentahydrate	24.97	100

The chemicals were dissolved in ASW water and kept at -4°C in stock solutions.

3.1.3 Fluorescent dyes

Three dyes were used to localise lipid droplets *in vivo*. Table 4 shows how dye stocks were obtained.

Table 4 Fluorophore stocks.

Fluorophore (Invitrogen)	**Stock**	**Amount used**		**Final concentration (mM)**
		Fluorophore/Stock	**Solvent**	
BODIPY 493/503	9.5 mM	0.5 ml	0.75 ml	4
FM4-64		5 mg	1 ml	5
DAPI				

BODIPY and FM4-64 were dissolved in dimethyl sulfoxide (DMSO, Sigma).

3.1.4 Nitrogen free ASW

Table 5 shows the formulation used to prepare 1L of nitrogen free ASW:

Table 5 Nitrogen free ASW (Harrison et al., 1980).

Anhydrous salts	**Amount (g/L)**	**Concentration (mM)**
Sodium chloride	20.756	362.7
Sodium sulfate	3.477	25.0
Potassium chloride	0.587	8.03
Sodium bicarbonate	0.170	20.07
Potassium bromide	0.085	0.73
Boric acid	0.022	0.37
Sodium fluoride	0.003	0.066
Hydrated salts		
Magnesium chloride*6H_2O	9.395	47.18
Calcium chloride*2 H_2O	1.316	9.134
Strontium chloride*6 H_2O	0.021	0.082

Anhydrous and Hydrated salts must be dissolved separately in DI water and mixed afterwards.

3.2 Algae collection and keeping

Ulva thalli were collected in Seaham, County Durham, England (54°50'25.25''N, -1°20'15.06'' W) and taken to the lab in excess seawater to reduce stress. Once in the lab, all the epiphytic organisms and materials were removed (*e.g*. shrimps, seashells, stones, dead parts) to ensure *Ulva* would be kept healthy. After that, thalli are put into beakers and topped up with artificial seawater (ASW) and put into incubation at 8°C and 90 rpm. ASW is changed every week.

3.3 Pathway elucidation and gene search

I reviewed the literature to identify the proteins involved in lipid droplet formation. The search focused on the microalga *C. reinhardtii* (Cr), because of its close phylogenetic relation to *Ulva* and its well characterised genome; *Arabidopsis thaliana* and other plant species were also investigated. The Web of Science database was searched for the words "Chlamydomonas" followed by "Lipid Droplet". The resulting 103 papers were scanned to find all the genes known to be related to lipid droplet formation. This list was then used to 'map' the enzymes in *C. reinhardtii*'s pathway (Figures 1 to 4). Those genes without a relevant function were discarded.

Once the list of putative genes was ready (Appendix 1), their amino acid sequences were searched in NCBI databases and literature. These sequences were then BLASTed against the *Ulva mutabilis* genome (Umu) (De Clerck et al., 2018) on the ORCAE server (https://bioinformatics.psb.ugent.be/orcae/). The final gene list (Table 5) was sent to Santiago de Chile University (USACH) where it was analysed for differential expression in *Ulva compressa*. *Ulva mutabilis* lipid droplet-related genes were BLASTed against the *Ulva compressa* transcriptome. Once the *Ulva compressa* lipid droplet genes were identified, qPCR was performed. Samples were taken at 0h, 3h, 6h, 12h, 24h to measure transcription.

3.4 Metal stress

3.4.1 Metal exposure to Lead and Copper

Ulva was exposed to metal stress for future confocal microscopy observations. Initially, the experiment was carried out with three conditions (Table 6). For each culture, an approximately 15 cm long section of thallus was put into beakers with 200 ml of ASW.

Table 6 Lead and Copper exposure experiment.

Culture	Metal Source	Metal source concentration
Control	-	-
Lead-treated	Lead acetate 10mM	10 µM
Copper-treated	Copper sulfate 100mM	100 µM

Metal was added to 200 ml of ASW, the final concentrations were obtained by adding 200 µl of stock solution (Table 2) into each culture. The cultures were kept for 48 h at 8 °C and 90 rpm. After this period, samples were prepared for fluorescence microscopy.

Then, to either confirm some results or to try different treatments, another experiment was carried out with four conditions (Table 7). Cultures were set up similarly to the previous experiment, using the glutathione (GSH) inhibitor, buthionine sulfoximine (BSO).

Table 7 Lead exposure experiment.

Culture	BSO	Lead acetate concentration
Control	-	-
Lead-treated	-	10 µM
Washout	-	10 µM
Lead + BSO treated	3mM	10 µM

To get lead acetate + Buthionine sulfoximine (BSO) culture, 130 mg of BSO were put in the culture media with the 200 µl of Lead acetate stock. The experiment was carried out over a 96-hour period as shown in Figure 6. All samples were incubated in ASW.

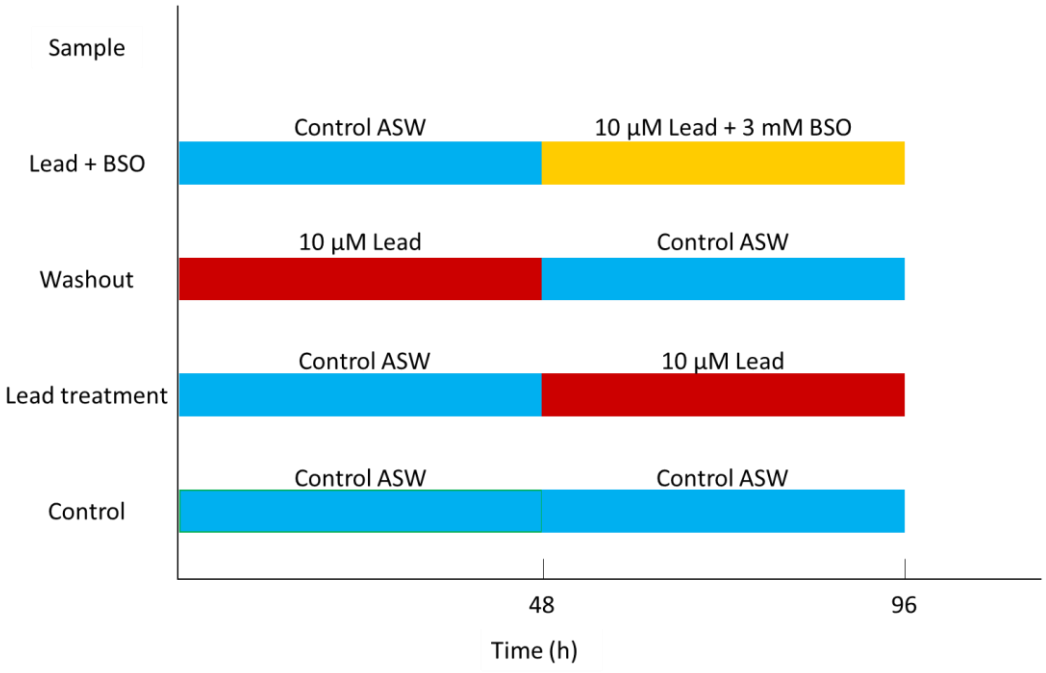

Figure 6 Lead exposure experiment design.

Moreover, a set of cultures was carried out to compare copper effects to lead ones and a BSO control was added to the experiment. The conditions for these experiments are shown in Table 8.

Table 8 Copper exposure experiment.

Culture	BSO	Copper sulfate concentration
Control	-	-
BSO Control	3mM	-
Copper	-	25 µM
Copper + BSO treated	3mM	25 µM

In this case, culture volume was 120 ml. 30 µl from Copper sulfate stock (Table 5) were added to copper-treated samples to get a 25 µM concentration.

3.5 Fluorescence microscopy

To observe lipid droplet dynamics, we imaged *Ulva* cells in a confocal microscope after metal stress exposure. Confocal fluorescence microscopy was chosen because it let us observe *Ulva*

cells *in vivo.* Three fluorophores were used for staining (Table 4). 4mM BODIPY 493/503 was selected to observe neutral lipids (lipid droplets). BODIPY is useful to label lipid droplets because of its lipophilic nature, which allows BODIPY to be incorporated into lipid droplets (Ohsaki, Shinohara, Suzuki, & Fujimoto, 2010; Suzuki, Shinohara & Fujimoto, 2012). DAPI to see the nucleotides and 5mM FM4-64 to try to label the vacuole. Immediately after the culture period finished, samples were prepared for fluorescence imaging. A small piece of algal tissue, of approximately $1cm^2$, was put into a petri dish with 5 ml of its corresponding culture media. Then, 20 µl of every dye stock solution was added. The samples were covered from light and left to stain for 30 min. After that, samples were sliced and mounted on a slide and covered with a coverslip before being placed in the microscope. Zeiss LSM 880 and a Leica TC5 SP5 (for copper experiment only) confocal microscopes were used.

The images taken were analysed using Fiji software (Schindelin et al., 2012; Rueden et al., 2017). The number and areas of lipid droplets were measured by drawing ellipses around each lipid droplet present in the cell. Data was then grouped into histograms. Only significant lipid droplets were taken onto account, leaving those with an area of $80nm^2$ or less out of the analysis. For the later copper experiment, quantitative analysis was not performed.

3.6 X-Ray diffraction (XRD)

In order to determine the presence of lead sulfide (PbS) in my samples, I ran an XRD analysis. For sampling I set up a culture for metal stress with a control sample and a lead treated one using the same lead source and concentrations shown in Table 5. After 48h of culture the samples were quickly frozen in liquid Nitrogen for later freeze-drying. After 48h in the freeze-dryer the samples were placed in the fridge (4°C) for storage.

To load samples in the X-Ray diffractometer, they were ground into a fine powder. Powdered samples were then sieved and sealed over a zero-diffraction silicon plate using high vacuum grease (Dow Corning). The external part of the plate was wiped to remove any sample excess and avoid damaging the X-ray diffractometer. The plates were then loaded on a Bruker D8 advance X-ray diffractometer and left for reading for 50 min. The intensities were measured from 10° to 80° 2θ angle using CuKα radiation.

4 Results

4.1 Pathway elucidation and gene search

Previous studies report that lipid droplet formation pathways are present in all organisms. (Pyc et al., 2017, Guo et al., 2009). Since lipid droplets are oil stores, they are an important key towards elucidating lipid metabolism in *Ulva*. This led me to hypothesise that identifying lipid droplet genes in model organisms would let us identify their homologues in our *Ulva mutabilis* genome (De Clerck et al., 2018). Once we knew which known lipid droplet regulatory genes were present in *Ulva*, we would be able to investigate the process more closely in this species, providing a base for the rest of my work.

Accordingly, we looked for known lipid droplet genes in the model organisms *Arabidopsis thaliana* and *Chlamydomonas reinhardtii*. The extensive studies in both species increases the probability of finding characterised genetic sequences. In addition, *C. reinhardtii* is closely phylogenetically related to the *Ulva* genus, which increases the likelihood of finding orthologous genes in *U. mutabilis*. I therefore performed a literature review to identify 36 lipid droplet-related genes in *Arabidopsis* and *Chlamydomonas* (c.f. § 7.1, Appendix 1) and BLASTed these against the *U. mutabilis* genome. We found homologs of 14 of these genes present in the *Ulva mutabilis* genome, known in other organisms to be involved in the diverse stages of lipid droplet formation.

These genes encode a total of 14 proteins: five acyltransferases (DGTT 1 and 2, GPAT, LPAAT2 and LPLAT), which are involved in TAG assembly (Zienkiewicz, Du, Ma, Vollheyde, & Benning, 2016; Kim, Terng, Riekhof, Cahoon, & Cerutti, 2018; Boyle et al., 2012; Goold et al., 2016; Manandhar-Shrestha & Hildebrand, 2015 and Nguyen et al., 2011). In addition, Plastid Galactoglycerolipid degradation 1 (PGD1) allows the accumulation of triacylglycerols (TAGs), which are later incorporated to lipid droplets (Goncalves, Wilkie, Kirst, & Rathinasabapathi, 2016). Citrate synthase (CIS), Acyl-CoA synthetase, Cyclopropane-fatty acyl-phospholipid synthase (CFA2) and Long-chain acyl-CoA synthetase (LCS2) are part of the earliest stages of fatty acid synthesis (Goncalves, Wilkie, Kirst, & Rathinasabapathi, 2016; Ramanan et al., 2013 and Goold et al., 2016). Trigalactosyldiacylglycerol 2 (TGD2) promotes lipid trafficking (Warakanont et al., 2015). Glycosyl hydrolase (GHL1) and DGTS Synthesis protein (BTA1) were reported to be present in isolated LDs from *C. reinhardtii* (Goold et al., 2016). Finally, Lipase 1

(LIP 1) promotes TAG turnover when Nitrogen is resupplied after deprivation. Table 9 shows the list of these lipid droplet genes. All the lipid droplet protein homologs found in *Ulva* were found from the *C. reinhardtii* genome and both sets of sequences are provided for comparison. The complete list of *C. reinhardtii's* lipid droplet proteins is provided in Appendix 1.

My list confirms that lipid droplet genes are widely conserved among species. However, further species-specific research is needed to take advantage of these pathways. For example, not all the genes known to be involved in lipid droplet formation in *C. reinhardtii* were found in *U. mutabilis*, which implies that *Ulva* may have evolved its own unique lipid droplet proteins. Some proteins, like DGTT 1 and 2, are also encoded by various sequences in each species, suggesting that regulation may differ from one species to another.

Table 9 Lipid droplet related genes in the Ulva genome.

Protein	**Protein name**	**Gene family (ORCAE)**	**Gene identifier (*Ulva*)**	**Gene name (*C. reinhardtii*)**
CIS	Citrate synthase	HOM02ULVA001071	Um00514_0009	CR09G07800
LIP1	Lipase1	HOM02ULVA000466	Um00105_0004	CR12G13380
ACS2	Acyl-CoA synthetase	HOM02ULVA000475	Um00197_024; Um00197_0242	CR01G02730
BTA1	DGTS Synthesis protein	HOM02ULVA005820	Um01035_0022	CR02G12960
CFA2	Cyclopropane-fatty acyl-phospholipid synthase	HOM02ULVA001391	Um00300_0024; Um00425_0001; Um00425_0002; Um00763_0010; Um01035_0022	CR07G02640
DGTT1	Diacylglycerol O-acetyltransferase type 2	HOM02ULVA000286	Um00598_0020; Um01000_0117; Um01000_0128	CR06G09280
DGTT2	Diacylglycerol O-acetyltransferase type 2 2	HOM02ULVA000139	Um00063_0057; Um00139_0035; Um00156_0022; Um00402_0010; Um01000_0019	CR03G06590
GPAT	Glycerol-3-phosphate acyltransferase	HOM02ULVA003414	Um01158_0012	CR06G13180
GHL1	Glycosyl hydrolase	HOM02ULVA000136	Um00236_0008; Um00203_0096	CR03G09140
LCS2	Long-chain acyl-CoA synthetase	HOM02ULVA000148	Um00086_0005; Um00203_0037; Um00203_0038; Um00463_0047; Um01004_0048	CR16G00410

LPAAT2	Chlorophyte specific Lysophosphatidic acid acyltransferase	HOM02ULVA001894	Um00636_0010	CR12G06870
LPLAT	Lysophospholipid acyl transferase	HOM02ULVA001363	Um01153_0039	CR12G05950
PGD1	Plastid Galactoglycerolipid degradation 1	HOM02ULVA000117	Um00021_0079; Um00081_0009; Um00289_0001; Um00291_0045; Um00337_0051	CR07G07710
TGD2	Trigalactosyldiacylglycerol2	HOM02ULVA003364	Um00141_0050	CR01G11880

4.2 Metal stress

To test my hypothesis that "Lipid droplets expand and multiply after metal exposure", I cultured *Ulva* thalli in metal-containing media. To observe the effects and compare metal-treated tissue with untreated *Ulva* thalli, each culture was stained with fluorescent dyes and prepared for confocal microscopy.

We chose copper and lead for our metal cultures because they are commonly found in metal-polluted seawater. To help dissect out the effects of metal elevations, I also cultured additional metal-treated samples with buthionine sulfoximine (BSO), an inhibitor of glutathione (GSH) synthesis. I reasoned that this inhibition of phytochelatin synthesis and, consequently, the disabling of one of the cell's main defences against metal, would shed additional light on lipid droplet formation mechanisms in response to stress.

Confocal imaging was chosen to allow me to observe and identify a broader range of lipid droplet dynamics. Lipid droplets do not remain static after their formation and they perform several roles besides lipid storage (Welte, 2015). Lipid droplets can fuse to increase their size, and their mobility contributes to cell transport because they can move around and bind to other organelles (Hashemi & Goodman, 2015).

4.2.1 Lead exposure

Images taken after culturing show an increase in the size and number of lipid droplets after high metal exposure (Figure 7) and the differences between treatments were quantified by counting and measuring BODIPY-labelled lipid droplets (Figures 9 and 10; box widths were determined according to Sturges' rule as in Scott, 2015).

From the histograms we could observe that lead and washout samples behaved as expected: the washout conditions showed that *Ulva* can recover from metal stress with the number of lipid droplets going back to those seen in control samples (Figure 9 A and D). Despite the presence of lead, BSO-treated samples presented fewer lipid droplets than the sample treated with only Lead (Figure 9 C and B).

Lipid droplet size was also affected by lead exposure. All the samples treated with lead (Lead-treated, Lead + BSO and Washout) present bigger lipid droplets than Control sample (Figure 10 A-D).

Lipid droplet dynamics were also observed. It was possible to spot two lipid droplets joining (Figure 11) confirming that typical lipid droplet dynamics were present. Moreover, Lead-treated samples showed an unexpected 'lipid vesicle' that moved quite rapidly into the part of the cell where we identified the vacuole in the light microscopy channel (Figure 12).

In addition, Lead+BSO image (Figure 7, Image C) shows 'spots' (highlighted in square) which were much bigger than average lipid droplets, (*e.g*. 6.7 μm^2, as opposed to ≈1 μm^2). Observations of these 'spots' on the light microscopy channel images (Figure 8A) let us identify a different structure, showing they are not lipid droplets. However, as they emitted a signal in the green channel just like BODIPY the next question arises: Is there another structure that stores neutral lipids besides lipid droplets?

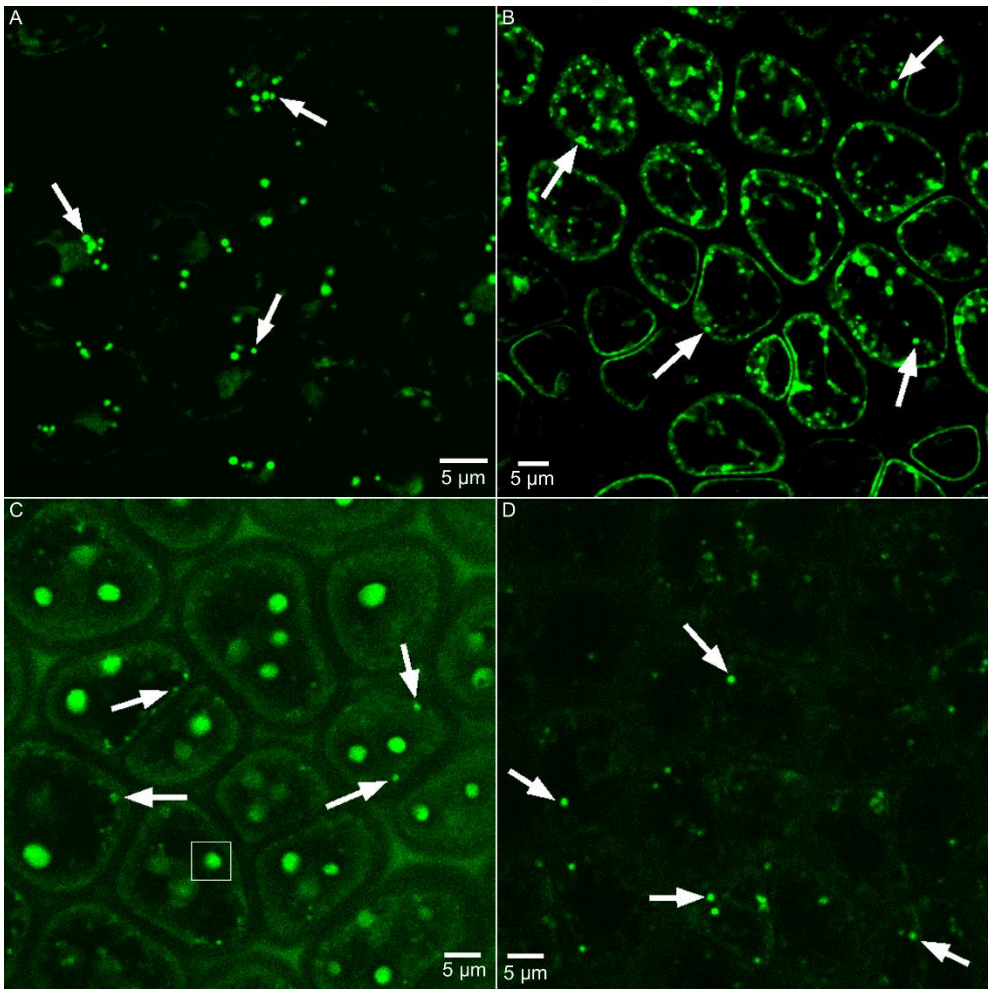

Figure 7 Lead treatment fluorescence imaging.

Fluorescence images showing the clear differences in LD (arrows) size and number for all the treatments. Being the Lead-treated sample (B) the one with the higher number of LDs as expected. In contrast, Control (A), BSO-treated (C) and washout (D) samples present fewer and smaller LDs. BSO sample (C) also shows the 'spots' (square).

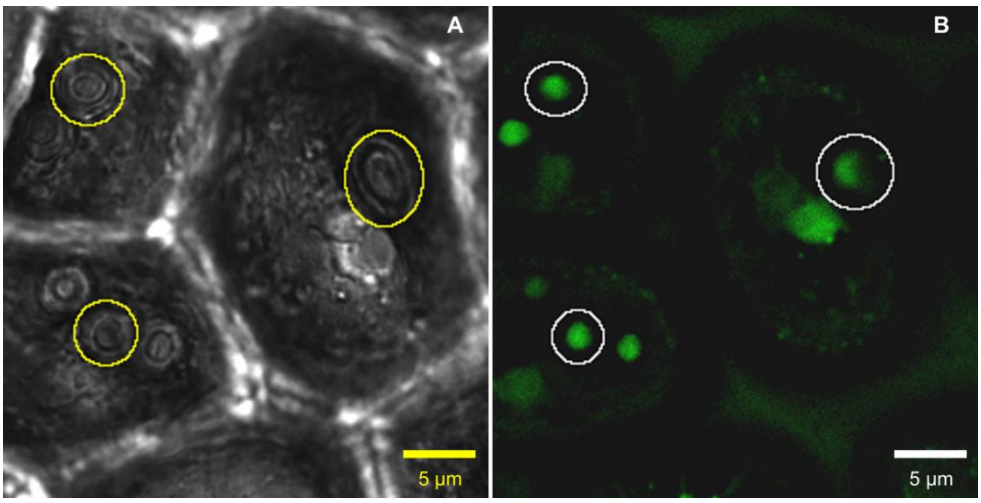

Figure 8 Larger spots.

Images that show the 'spots' (circles). Image A was taken from the Light microscopy channel. Image B was taken from the green channel (BODIPY)

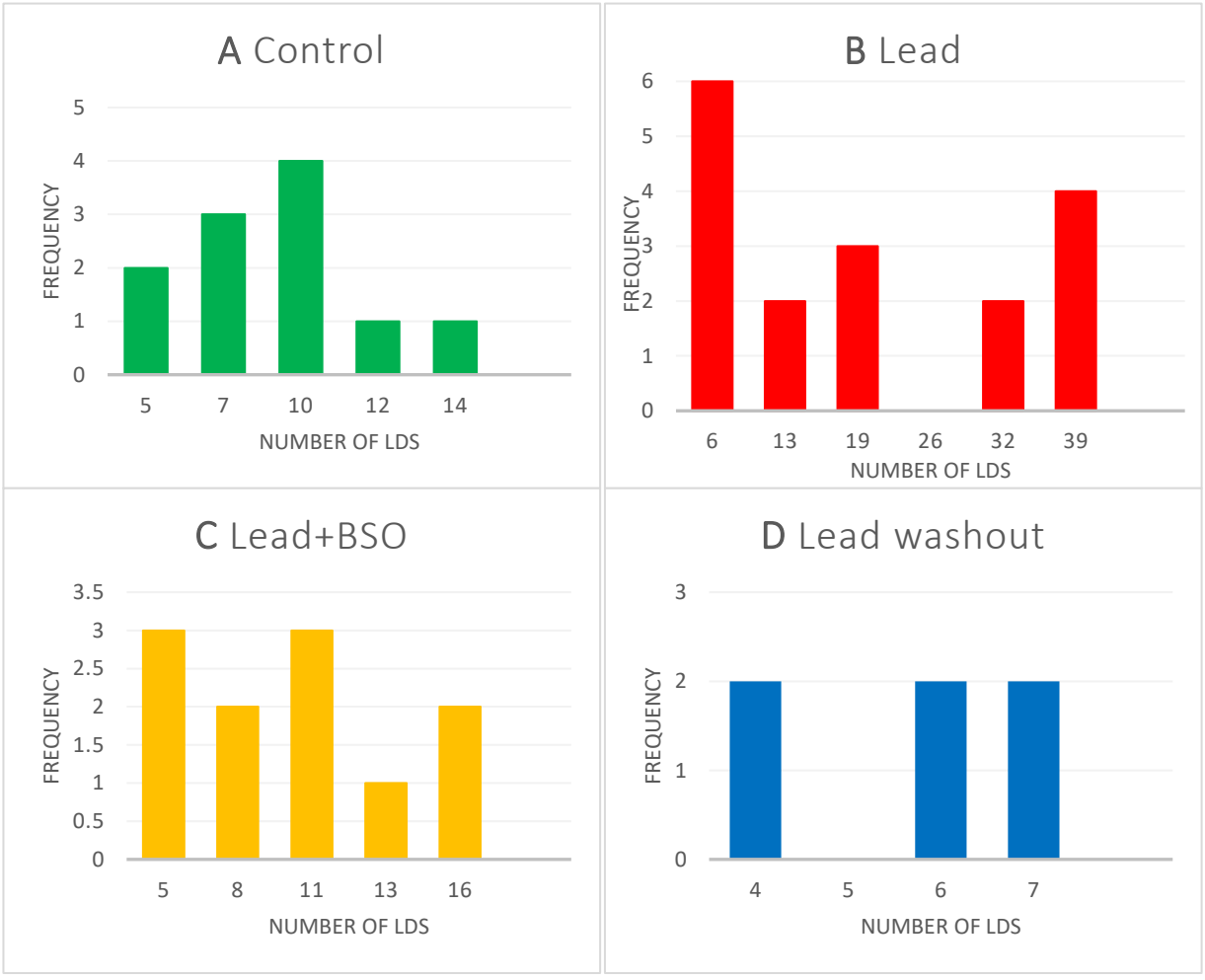

Figure 9 Number of LDs.

Histograms showing the lipid droplet number distribution on each sample. Clearly, lead treated cells (B) present a major LD number than the rest of samples. LD number in washout treatment (D) goes back to normal after lead exposure. The counts were performed once for each sample.

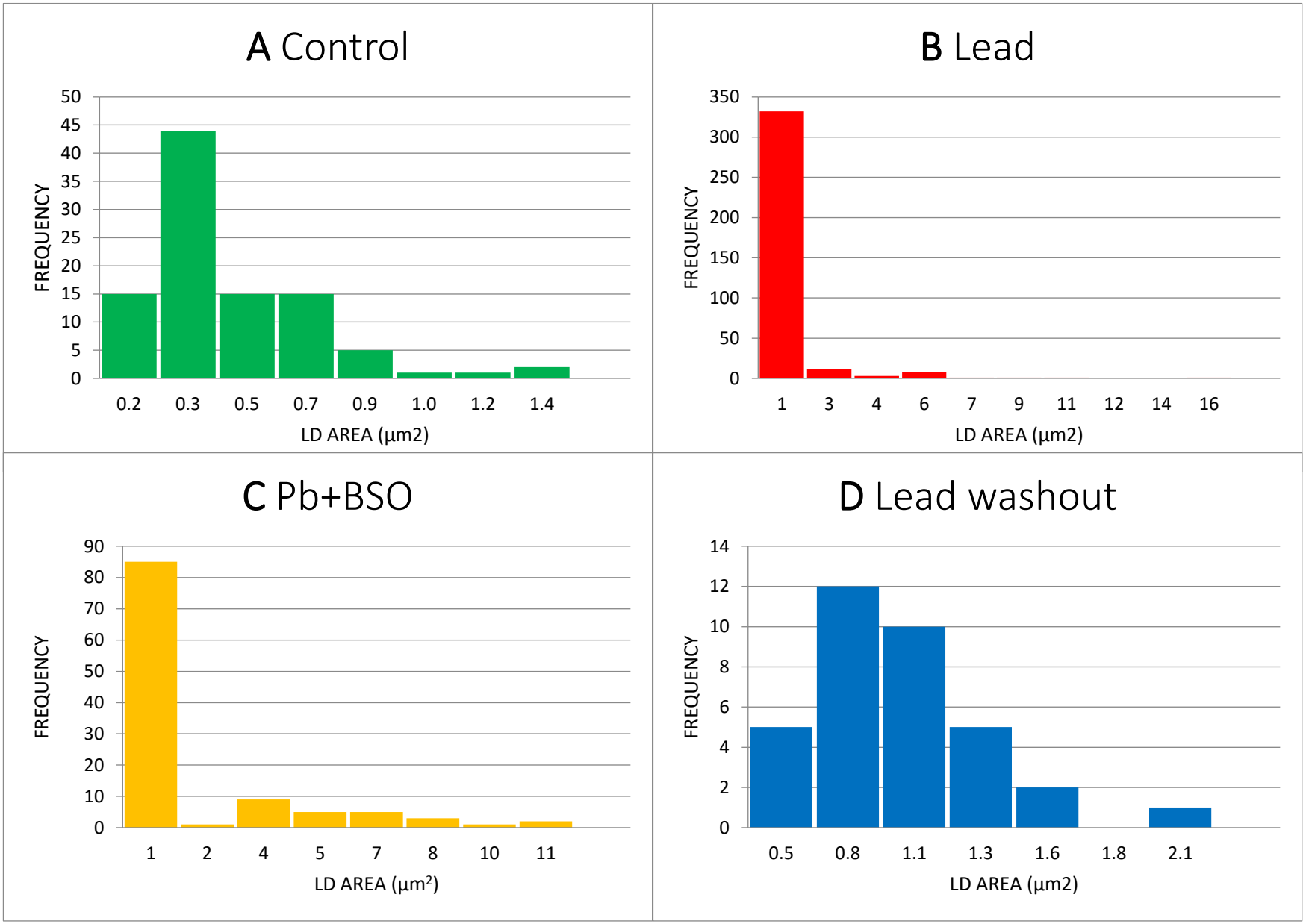

Figure 10 Lipid droplet size. Histograms showing the different sizes present in cells of all the four treatments. Control sample (A) presents the smallest size of LDs. These histograms include data from one measuring after removing the values corresponding to the 'larger spots' (see text for details).

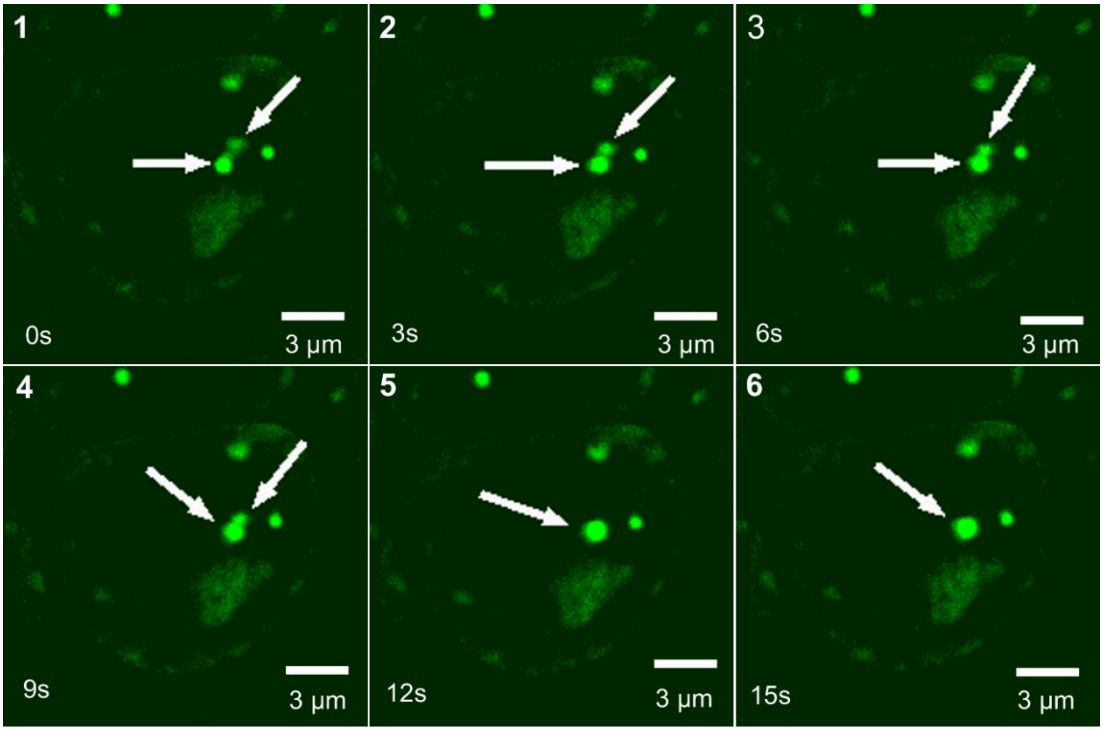

Figure 11 Lipid droplets joining.

LD joining process step by step. Image 1 shows the initial take. Joining and splitting is part of the typical LD life cycle. Indicative times are shown on each image.

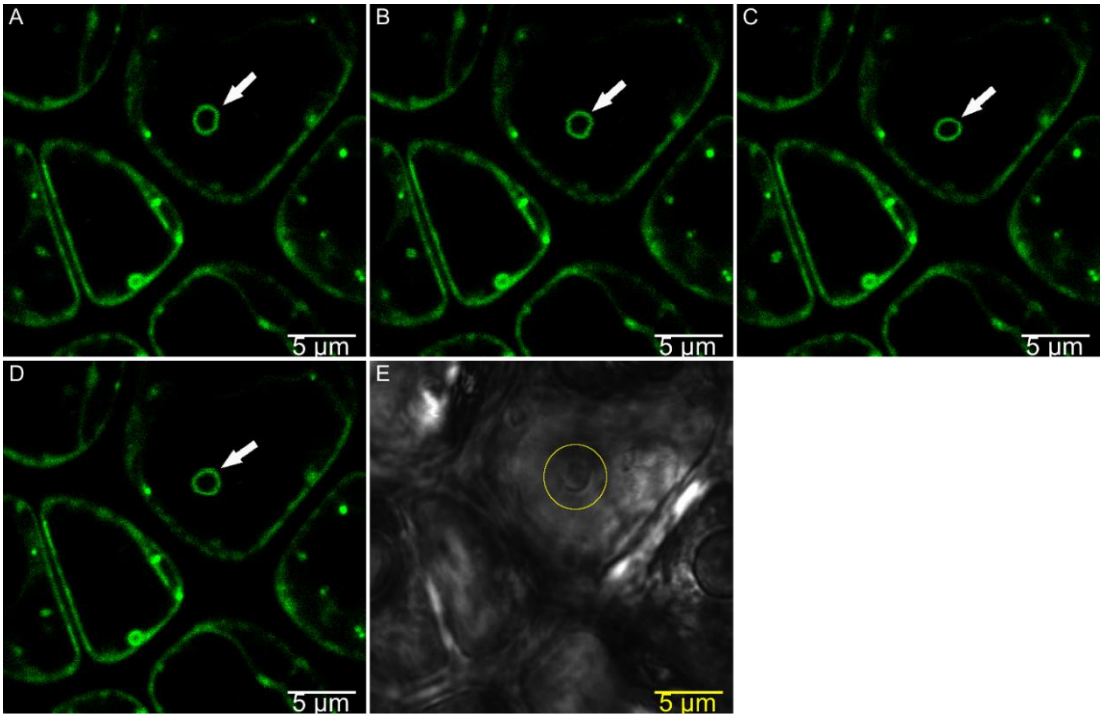

Figure 12 'Lipid vesicle'. Images A-D show four consecutive shots from live imaging. Panel A is the first position of the vesicle. Image E shows the vesicle observed in the light microscopy channel.

4.2.2 Copper exposure

Since the preliminary copper treatments caused cell death presumably due to high metal concentration (100 µM), this second treatment was carried out using a lower concentration (25 µM). Copper-treated cells showed similar behaviour to lead-treated ones; lipid droplets increased in size and number. This time fewer samples were observed and only the BODIPY channel signal (green) was considered (Figure 13). Lipid droplet measuring and counting were not done as we were more interested in qualitative change. In addition, copper-treated samples show the big spots observed in previous images (cf.§ 4.2.1 Figures 7 and 8).

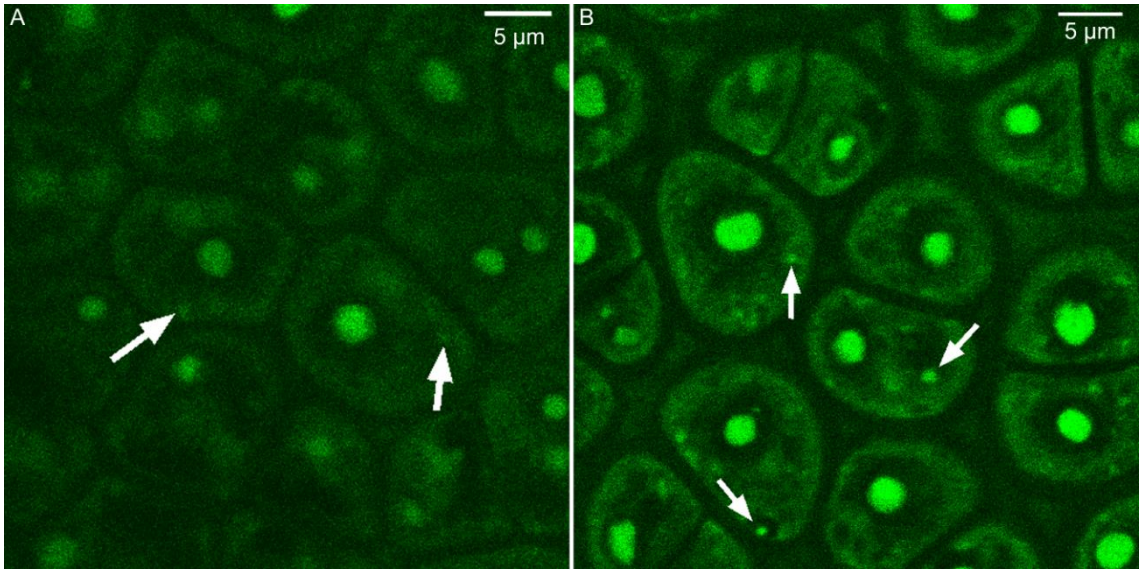

Figure 13 Copper exposure images.
Control sample (A) shows fewer LDs (arrows) than the Copper-treated sample (B).

In conclusion, fluorescence microscopy images demonstrated that metal treatment augments lipid droplet formation in *Ulva*. Our images also showed that typical lipid droplet dynamics, like mobility and fusing, are present in *Ulva*. However, several questions remain unanswered: most immediately. our 'spots' need to be characterised to determine what they are and whether they play a role in metal handling.

4.2.3 X-ray diffraction (XRD)

Marine organisms have developed diverse metal-handling mechanisms. Converting metals into phosphates, sulfides, carbonates or sequestering them in small proteins are common defence processes (Seshadri, Saranya, & Kowshik, 2011). Since *Ulva* performs an important

role in marine sulfur cycles (De Clerck et al., 2018), we hypothesised that lead sulfide formation could be one mechanism used by *Ulva*.

To test this hypothesis, I carried out X-Ray Diffraction (XRD) studies on control and metal-treated samples, hoping to identify metal salts from their characteristic diffractograms. My results showed that XRD patterns for my two analysed samples looked very similar (Figure 14). Both patterns show peak intensities for the following 2θ values: 27.7°, 28.2°, 28.5°, 31.8°, 40.7°, 56.5°, 66.4°, and 75.5° (Figure 14 A and B). Among the few differences found, an increase in diffraction intensity at 28.2° (Figure 14 B, labelled with an arrow) for lead-treated sample caught our attention. The peak generated at this diffraction angle is almost twice as high as in my control sample and draws the attention because this value is consistent with one of the characteristic 2θ values for a common lead salt: lead sulfide (PbS). Commonly, PbS diffracts around 29.96° (Bai & Zhang, 2009; Kalita et al., 2012; Seshadri, Saranya, & Kowshik, 2011). To be sure we were identifying lead sulfide and not another lead-sulfur compound (e.g. lead sulfate) the patterns obtained were also compared with lead sulfite ($PbSO_3$) and lead sulfate ($PbSO_4$); none of these seem to correlate with our spectra as well as PbS.

However, my results are suggestive, but not conclusive. My samples were not washed out after culturing, so it is likely that the rest of the diffractogram peaks (31.8°, 40.7°, 56.5°, 66.4°, and 75.5°) represent Sodium chloride (NaCl) and potassium chloride contamination from seawater in my sample; this will be covered further in my discussion section (c.f. § 5.5).

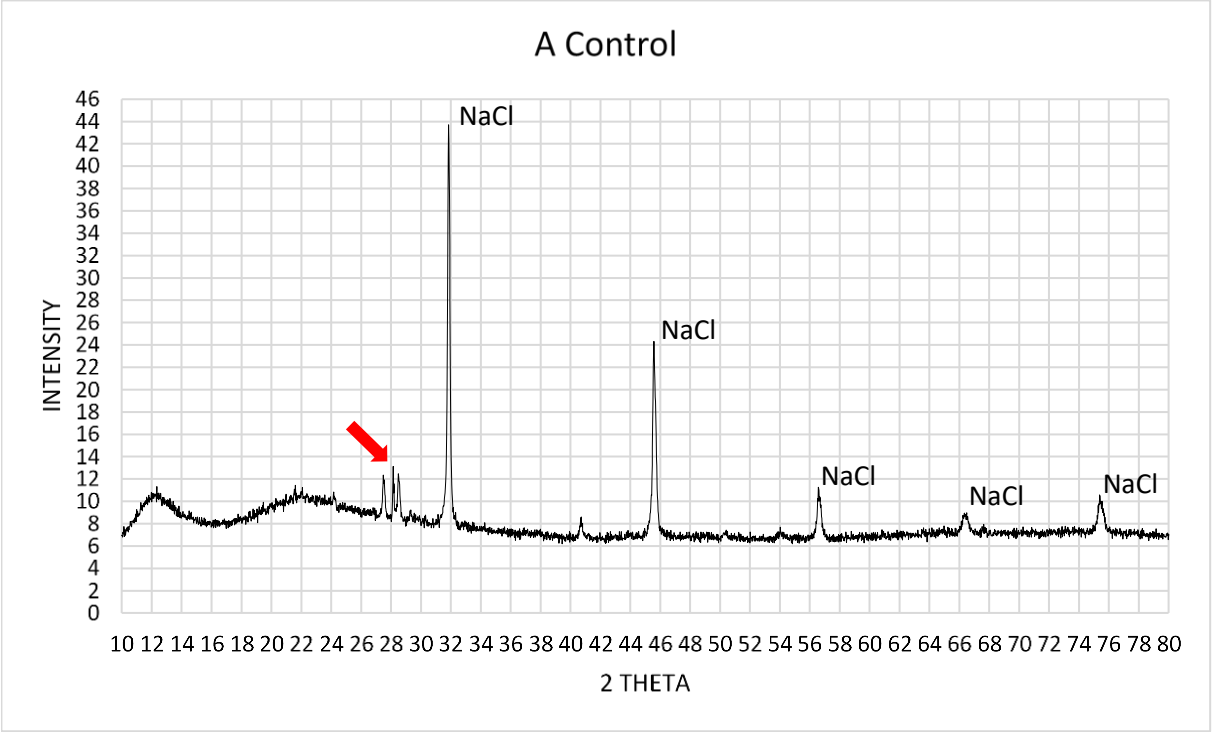

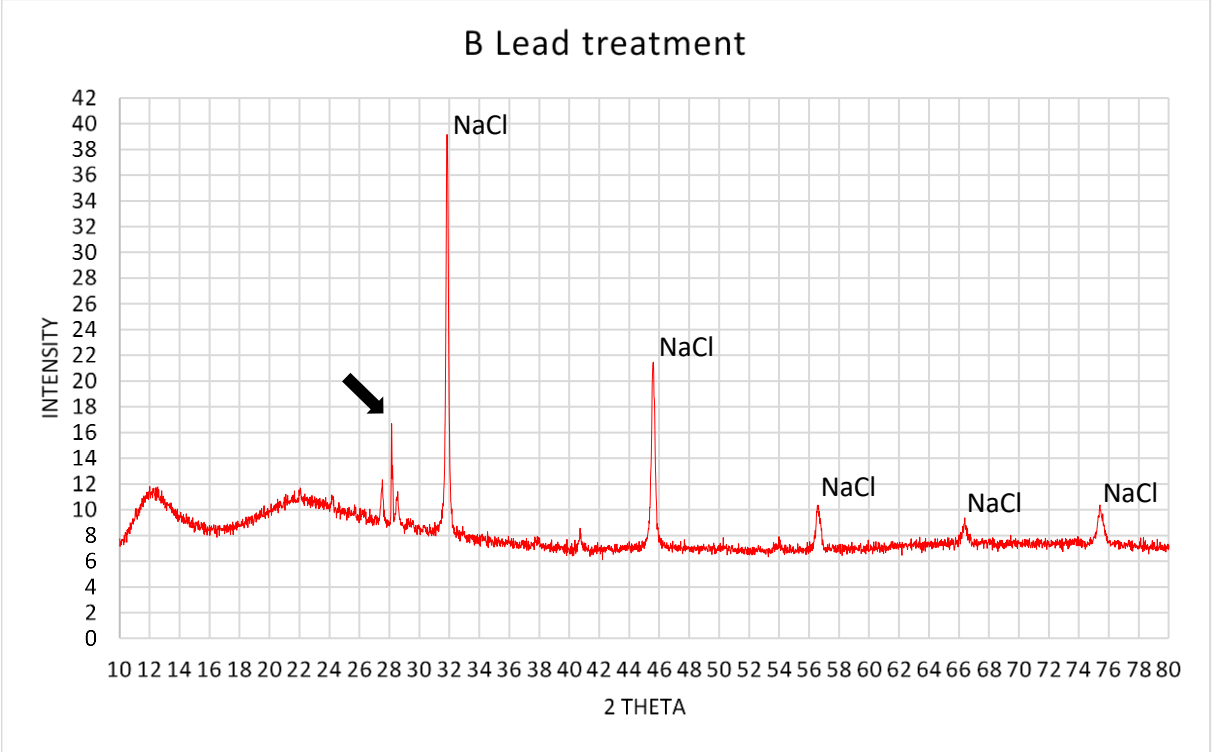

Figure 14 XRD patterns.

XRD patterns for indicative diffraction in Control sample (A) and Lead-treated sample (The red arrow shows the peak that we have tentatively identified as PbS for the control and the black arrow shows the same peak in the lead-treated sample. The highest peak (circle) in both cases corresponds to a Sodium (Na) signal (Grass & Stark, 2005; Li, Chen, Zhou, Gu, & Chen, 2005; Linnow, Zeunert, & Steiger, 2006; Rasmussen, Jørgensen, & Lundtoft, 1996).

5 Discussion

5.1 Pathway elucidation and gene search

From the literature review, I found 36 lipid droplet genes present in *Chlamydomonas reinhardtii* genome. Only 14 of them were identified in the *Ulva* genome. This suggests that core lipid droplet proteins share functions between species, but that each organism also has its own proteins that may modulate core lipid droplet genes.

Given the high diversity between algal species, it is necessary to broaden the knowledge we have about them, considering that each species may have significant differences in enzymes and pathways (Liu & Benning, 2013). For example, the Major Lipid Droplet Protein (MLDP) which has been reported in *C. reinhardtii* (Moriyama, Toyoshima, Saito, Wada, & Sato, 2017) was not found in the *U. mutabilis* genome and it seems not to be present in any macroalgal genome. To start elucidating a lipid droplet pathway for *Ulva*, I used my list of genes to map the enzymes found in the *U. mutabilis* genome according to their putative function. From this mapping I can propose a model for this process in *Ulva,* which is shown in Figures 15, 16 and 17.

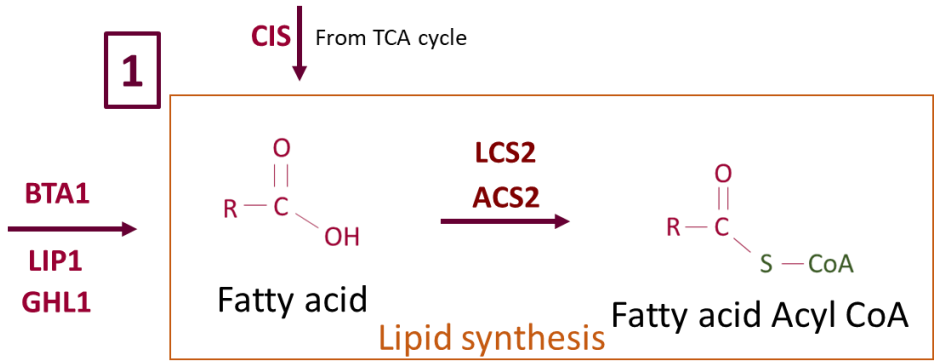

Figure 15 First stage of lipid droplet formation. Lipid synthesis.
Fatty acids (FA) which can be synthesised or obtained from cell membranes, are transformed into FA Acyl CoAs. Citrate synthase (CIS) regulates these reactions by redirecting Acyl CoA from the TCA cycle to lipid synthesis. See text for details and abbreviations.

The whole process can be divided into 3 clear stages: lipid synthesis, TAG synthesis and finally lipid droplet assembly. Lipid synthesis starts with the obtention of fatty acids (FAs), possibly via DGTS Synthesis protein (BTA1), Lipase1 (LIP1) or Glycosyl hydrolase 1 (GHL1) action (Figure 15). Fatty acids are then transformed into Acyl-CoAs by Acyl-CoA synthetase (ACS2) or Long-

chain Acyl-CoA Synthetase (LCS2). Some enzymes have been demonstrated to be indirectly involved in the process, like Citrate synthase (CIS), which regulates TAG synthesis by redirecting Acyl-CoA from TCA cycle to fatty acid synthesis when deactivated (Deng, Cai, & Fei, 2013). The endoplasmic reticulum and the chloroplast have been proposed as the location of this first stage in the well-studied *C. reinhardtii* (Zienkiewicz, Du, Ma, Vollheyde, & Benning, 2016). Despite the evolutionary differences between algal species, *C. reinhardtii* has a close phylogenetic relation with *Ulva*.

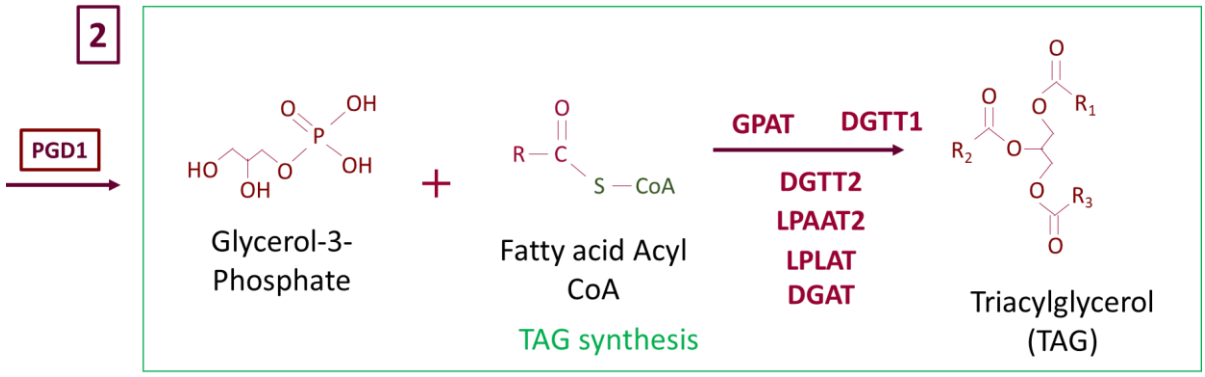

Figure 16 Second stage of lipid droplet formation. TAG synthesis.
In the cytosol, Fatty acid Acyl CoAs are incorporated into Glycerol-3-Phosphate (G3P) via Acyltransferases (GPAT, DGTT1 and 2, LPAAT2, LPLAT or DGAT) action until G3P is transformed into a Triacylglycerol. See text for details and abbreviations.

During the next stage of the model (Figure 16), this excess of lipids is transformed into triacylglycerols (TAGs). The lipids can come from lipid synthesis or from degradation of membranes via Plastid galactoglycerolipid degradation (PGD1). Acyltransferases (*e.g.* DGTT, DGAT) play a major role in TAG synthesis. It is important to note that most of the genes found for this work were acyltransferases (see cf.§ 5.1 Table 9 and Appendix 1). They are responsible for transforming glycerol and fatty acid-Acyl CoAs into TAGs. The *C. reinhardtii* encodes 6 diacylglycerol acyltransferases (DGATs). This suggests that TAG synthesis is an important process in this *Chlamydomonas'* metabolism. In addition, the variety of DGATs may suggest that each of them is involved in a different process, such as a specific stress response. In fact, Pugkaew et al. (2017) mention that DGTT1 increases its expression after Nitrogen depletion while DGTT2 does it after exposure to rapamycin. Therefore, a broader and deeper metabolic

study of other algal species like the macroalgal *Ulva* genus is necessary; comparison of various stress responses via expression analysis may confirm this.

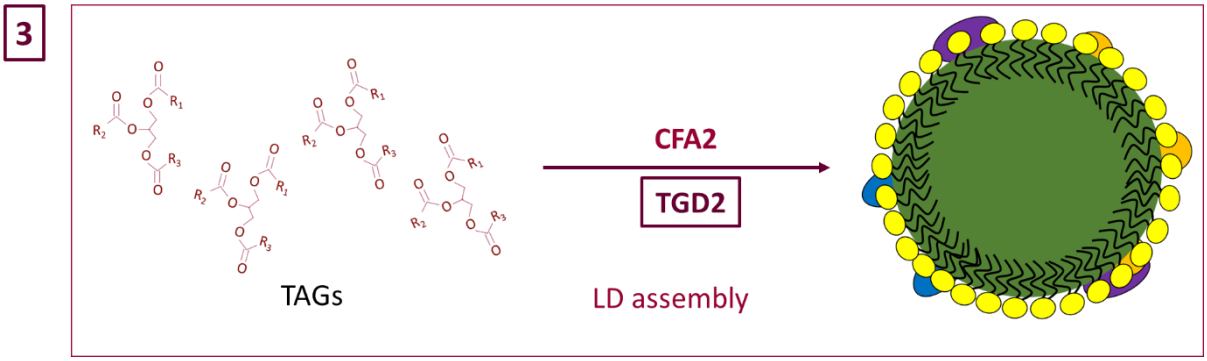

Figure 17 Third stage of lipid droplet formation. LD assembly.
TAGs are transported into the growing LD by transporters (e.g. TGD2) action. Other proteins like Cyclopropane fatty acid synthase (CFA2) are responsible for synthesising phospholipids for the monolayer and attaching other membrane proteins. See text for details and abbreviations.

In the last stage of the model, lipid droplets would be formed or would increase their size to store the excess of TAGs. Triacylglycerols are transported to the growing lipid droplet by a lipid carrier like Trigalactosyldiacylgliycerol (TGD2), while Cyclopropane fatty acid synthase (CFA2) synthesises the phospholipids to increase the monolayer diameter (Figure 17). Simultaneously, proteins like acyltransferases, membrane traffickers, an equivalent to microalgal Major Lipid Droplet Protein, lipid synthesis enzymes, and maybe transporters are incorporated to the surface of the lipid droplet to ensure it accomplishes its function within the cell (Guo et al., 2009). Since algal lipid droplets have not yet been widely studied, a deeper characterization is still needed. Extracting them to characterise the type of lipids kept inside, protein labelling to identify lipid droplet proteins (*e.g.* with antibodies or fluorescent dyes) as well as deeper genetic comparisons may shed some light into macroalgal lipid droplet composition and function (Davidi, Katz, & Pick, 2012; Suzuki, Shinohara & Fujimoto, 2012).

5.2 Differential expression

Starting from the hypothesis “Metal stress increases lipid content” we expected an increase in the expression of any of the genes related to fatty acid synthesis or such as BTA1 or ACS2 (Figure 15). In fact, Ramanan and collaborators (2013) reported acetate as a key factor in lipid droplet synthesis. In their work, they triggered lipid droplet formation by exposing a starchless

C. reinhardtii strain to nitrogen starvation, a quite common type of stress. Hence, ACS2 would be a good candidate to overexpress after metal exposure.

During TAG synthesis, genes like Diacylglycerol acyltransferase type 2 (DGTT) and Phospholipid diacylglycerol acyltransferase (PDAT1) have been demonstrated to overexpress in *C. reinhardtii* cells after nitrogen starvation (Boyle et al., 2012). In Boyle and collaborators' research, DGTT1 was also proven to increase its expression after exposing *C. reinhardtii* cells to sulfur and phosphorous starvation. Therefore, an increase in DGTT1 and PDAT1 transcription would also be expected (Figure 16).

Finally, TAGs would then accumulate and later become into the core of a lipid droplet during the third step of the proposed pathway. Once again, a higher transcription of lipid synthesis enzymes as well as lipid transporters would support our model and bring us closer to understanding *Ulva´*s lipid metabolism after metal exposure.

Surprisingly, differential expression results sent from Chile indicate that our first hypothesis may need to be rethought. We found that, during metal exposure, the proteins responsible for synthesising new lipids did not increase their genetic expression. Instead, the proteins which significantly increased their expression were those responsible for lipid hydrolysis and lipid transport; PGD1 and TGD2. Hence, the hypothesis that stated "Metal stress increases lipid content" is not supported. Consequently, I suggest an alternative hypothesis: the lipids inside the cell redistribute instead of being synthesised *de novo*. What might be happening is that the lipids present in other parts of the cell, for example in cellular membranes, are pulled to TAG synthesis and accumulated in lipid droplets. Metal stress increases Reactive Oxygen Species (ROS) accumulation in the cell (Moenne, González, & Sáez, 2016). The increased oxidation may cause membrane disruption and lipid lysis, probably effected by Plastid Galactoglycerolipid degradation 1 (PGD1) in our model, releasing fatty acids (FAs) which are then used to synthesise TAGs and then transported into lipid droplets putatively via Trigalactosyldiacylgliycerol 2 action. The increase in the transcription of PGD1 and TGD2 is consistent with this new hypothesis.

5.3 Metal stress

5.3.1 Lead and copper exposure

Although Lead and washout samples behaved as expected (Figures 9 and 10, § 4.2.1), we still observed some unexpected but interesting behaviour. On one hand, according to the hypothesis "Lipid droplets expand and multiply after metal exposure", a significant increase in the number of lipid droplets was perceived between the Control sample and the Lead-treated one. On the other hand, fluorescence images and lipid droplet counting data showed that Lead + BSO treatment resulted in fewer lipid droplets than expected. Buthionine sulfoximine (BSO) is a Glutathione (GSH) synthesis inhibitor (Griffith and Meister, 1979). Glutathione is a phytochelatin whose role in the cell is to sequester heavy metals (*e.g.* lead). In this way, GSH protects the organism against metal damage. Given GSH's role in metal handling, BSO was added to test its influence (if present) on lipid droplet mechanisms. While adding BSO to the experiment, we predicted that inhibition of Glutathione (GSH) synthesis would not affect lipid formation, localisation, or dynamics.

Unexpectedly, BSO-treated *Ulva* presents fewer lipid droplets than *Ulva* treated with only lead. This suggests that lipid droplet formation and heavy metal chelation, two metal-handling mechanisms that we thought would be independent, may be under common regulatory control yet unknown. This is further evidence that metabolic studies in *Ulva* are essential to determine its suitability as a biodiesel source.

Besides metal-induced lipid droplets, fluorescence imaging let us observe lipid droplet dynamics. As mentioned above (c.f. § 4.2.1, Figure 11), we could see a couple of lipid droplets joining. Since we relate lipid droplets to metal handling, we suspected lipid droplets would move quickly inside the cell in order to decrease metal concentration as soon as possible. Surprisingly, lipid droplets did not seem to move as rapidly as we expected; the live imaging of lipid droplets joining, as well as the rest of the images we collected show a slow movement (≈ 1 µm/min). We also observed another interesting phenomenon: fluorescence live imaging let us spot a 'lipid vesicle' (c.f. § 4.2.1, Figure 12). This vesicle moved more quickly than lipid droplets alone and it was easy to see it move out of the plane of focus and back in (Figure 18). Images taken from the light microscopy channel let us locate this vesicle in the vacuole, although this location was putative. We later confirmed this location while observing similar

structures in Transmission Electron Microscopy (TEM) images taken from a previous metal treatment which was part of another research project developed by our team (Figure 19).

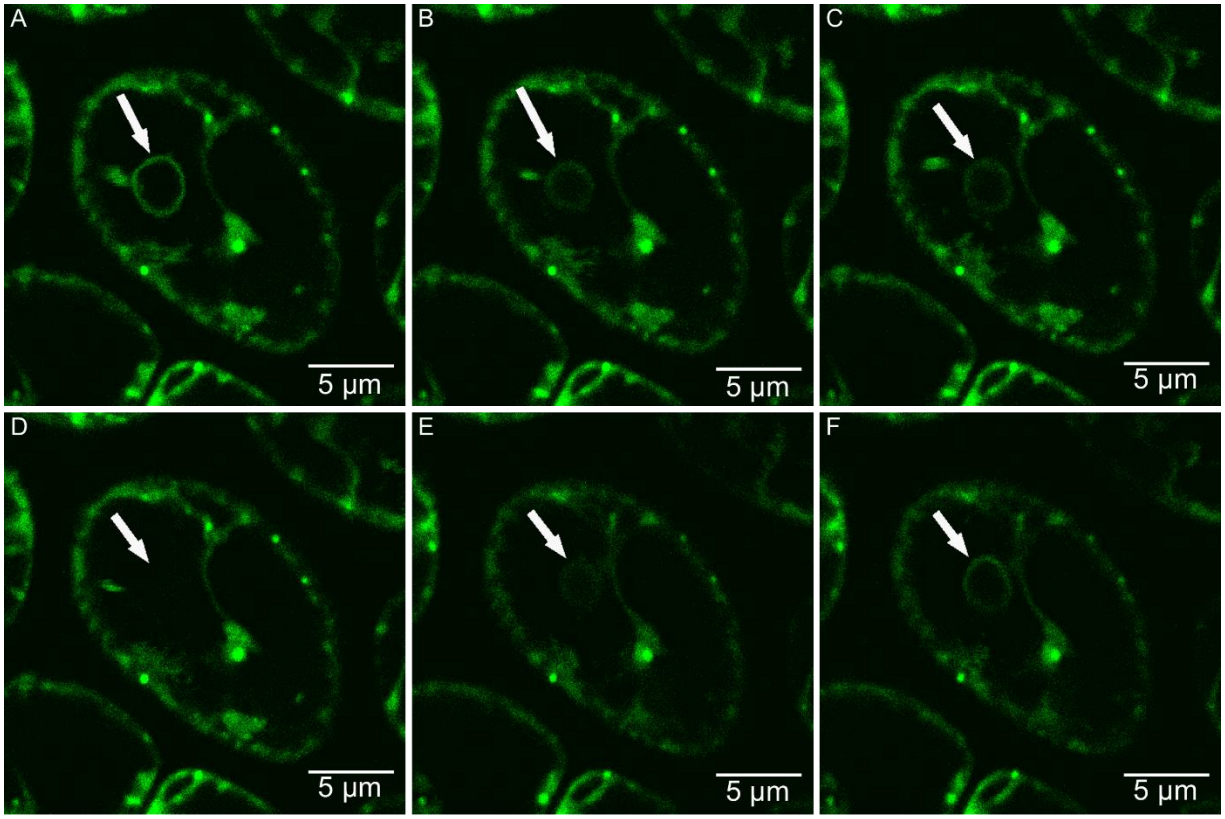

Figure 18 Lipid vesicle b).
This figure shows different shots from live imaging where the lipid vesicle is noticeable. Image A illustrates the first position of the lipid vesicle. Images C, D and E show the lipid going out of focus and back.

Moreover, observations in TEM images also gave us an indication of the electron density of these vesicles. It is possible to notice in Figure 19 that even though the lipid vesicles do not present a remarkable electron density, they may look darker than other membranes. This may indicate that lipid droplets also sequester and carry lead into the vacuole for disposal. This suggestion is supported by Andrade, Farina, & Amado Filho´s work (2004) on *Enteromorpha flexuosa*. They report an increase in lipid droplet formation, a higher number of vacuoles and some vesicles inside the vacuole after Copper exposure. In addition, Silverberg's publication about lead localisation in the green alga *Stigeoclonium tenue* (1975) mentions that lead is mainly deposited in the vacuole. Andrade and collaborators also report structural changes like membrane disruption, multiplication of starch granules and the increase of electron dense aggregates. We spotted the same changes in our TEM images (Figure 20). The observation of

lipid disruption is consistent with the new hypothesis we formulated based on our results (§ 5.2): lipids may be relocated from membranes to lipid droplets. Thus, the changes in the vacuole give us a hint about the role lipid droplets are playing during metal handling: lipid droplets are probably sequestering and transporting metals to the vacuole, reducing metal concentration in the cytoplasm.

Besides the expected changes caused by metal exposure and the unexpected information we have obtained, fluorescence imaging also showed another intriguing structure. Lead+BSO treatment images present extraordinarily big "lipid droplets" (Figure 8). In the beginning, the larger 'spots' were measured and counted as lipid droplets. However, after more thought, it was noticed that these spots were not present in the other lead-treated samples. This and the unusual size made us think they may be not lipid droplets. Hence, we tried to figure out what else could be emitting fluorescence in BODIPY channel.

To do so, we went back to light microscopy images and compared them with the fluorescence ones to try and identify the unknown spots. The most likely candidate is the pyrenoid: a structure located in the chloroplast. They are involved in CO_2 fixation and are mostly composed by Ribulose bisphosphate carboxylase/oxygenase (RUBISCO). They can grow and multiply as algal cells grow older (Teng, Ding, & Lu, 2011). This last fact is consistent with the number of 'spots' seen in each of our cells. Despite the similarity of our images to actual pyrenoids (Figure 21), the reason why they emit fluorescence in the green channel (BODIPY signal) remains unknown.

Since pyrenoids are located in the chloroplast, chlorophyll's autofluorescence may be related to the pyrenoids' capacity to emit a signal (Kodama, 2016). Moreover, it is reasonable to consider that pyrenoids have different staining properties than the rest of the chloroplast (Gibbs, 1962). Therefore, it is feasible that they may contain an unidentified autofluorescent compound. As an alternative explanation, pyrenoids may be stained by BODIPY. They have been associated with oil synthetis in diatoms (Bose, 1941; 1943). Bose (1943) mentions healthy cells did not present oil droplets near the pyrenoid. Hence, is not unreasonable to think stressed cells' pyrenoids may be affected by metal stress, causing them to synthesise neutral lipids.

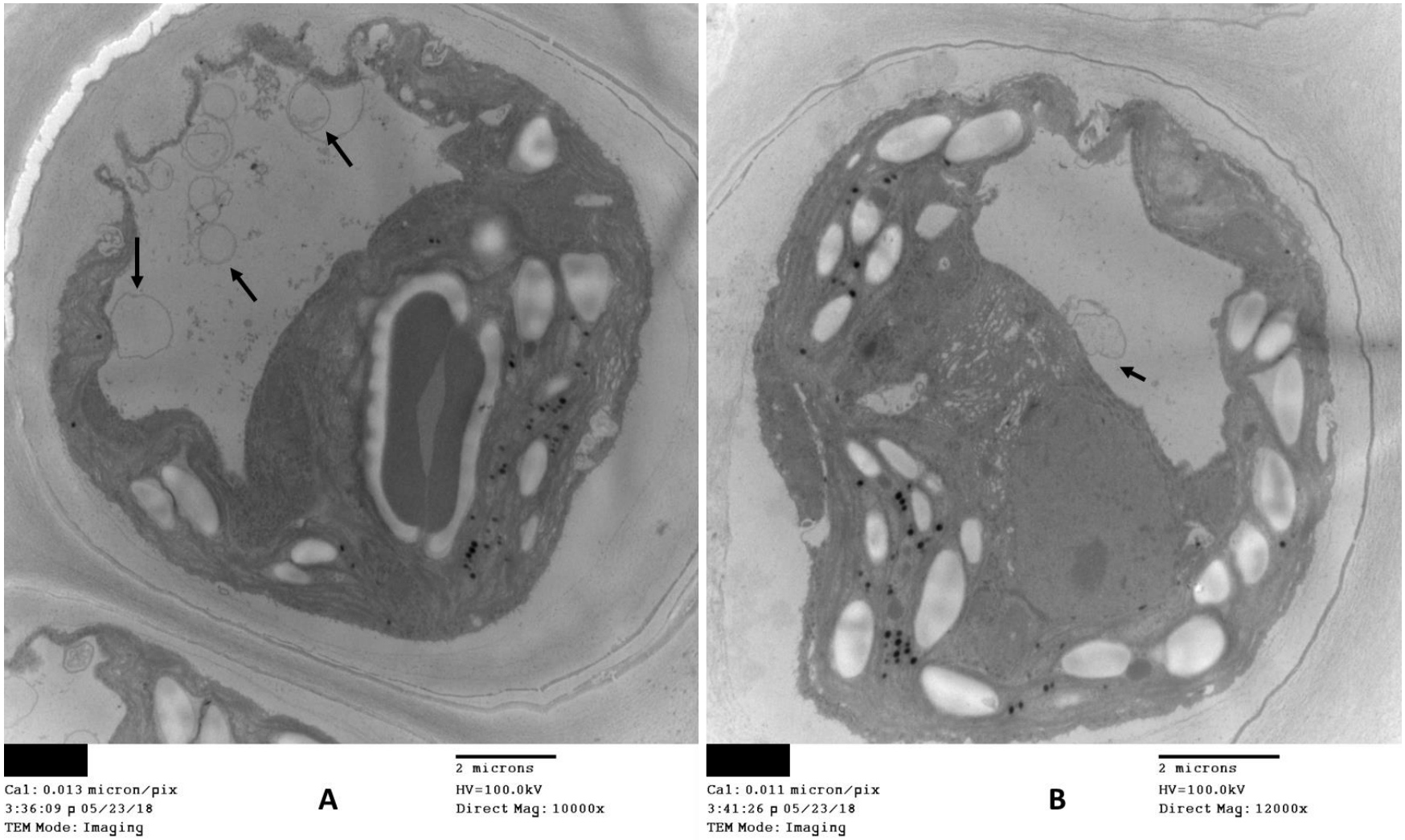

Figure 19 TEM lipid vesicle. TEM images showing 'lipid vesicles' (arrows) located in the vacuole of two different Lead+BSO-treated cells.

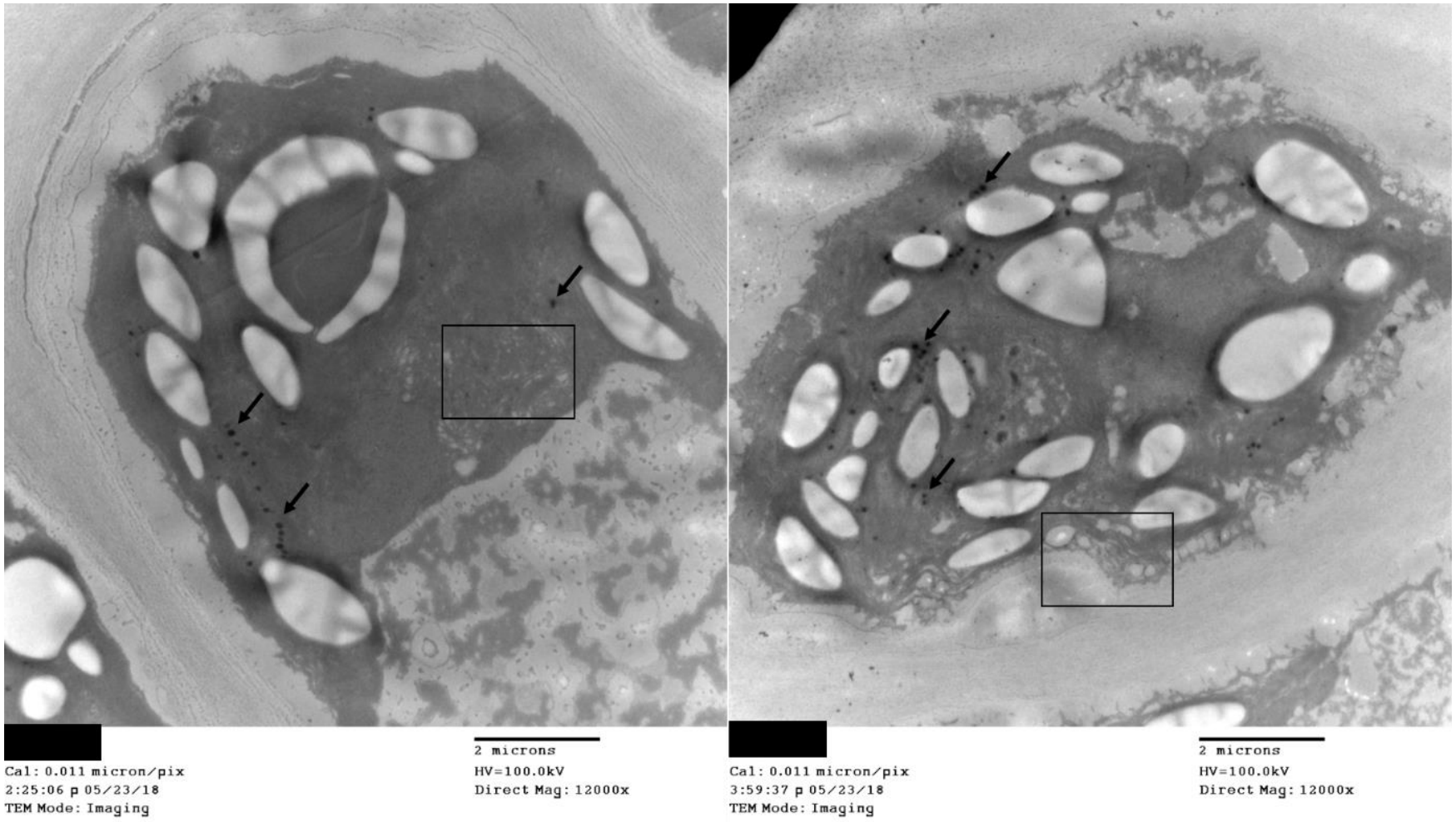

Figure 20 Cell morphology before and after metal. TEM images comparing the morphology of Control sample (A) and Pb-treated sample (B). In B it is possible to observe a higher number of electron dense aggregates (arrows) than in A. Also, it is noticeable that there is more membrane disruption in lead- treated sample when compared to control sample (squares). Major production of starch granules is also evident (S).

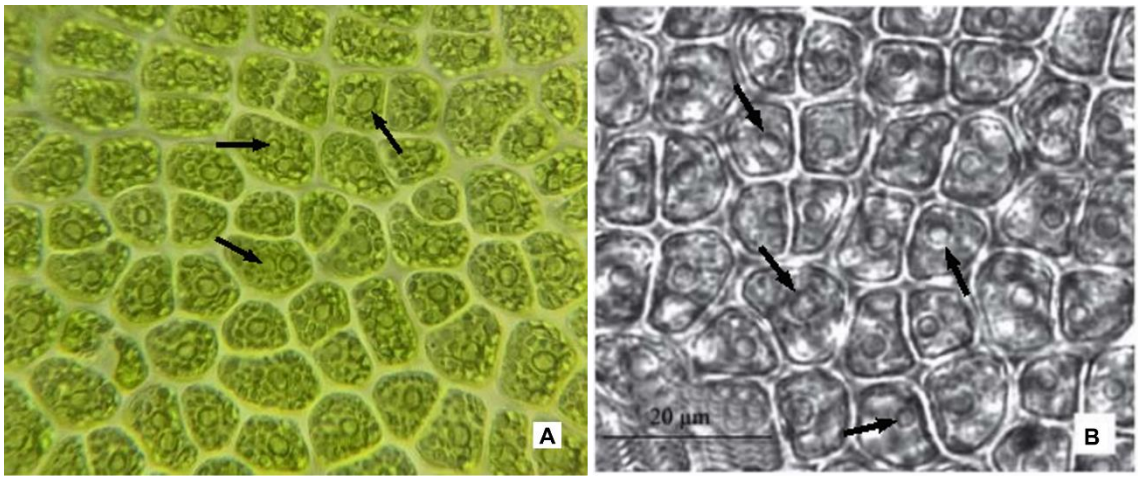

Figure 21 Pyrenoids comparison.
Picture A shows pyrenoids in *Ulva spp*. cells (pointed with arrows). Picture B shows the same organelle in *Enteromorpha linza*.

5.4 New Hypotheses

Taking all our results together, we took our initial hypothesis: "Metal stress increases lipid in *Ulva* cells" and reformulated it. Based on the differential expression analysis and the membrane disruption observed in TEM images, we can suggest that lipids are not synthesised *de novo* inside *Ulva* cells following metal stress and instead they are being relocated from cell membranes (*e.g.*, the chloroplast) and pulled into TAG synthesis by of oxidative stress. Studying the expression of desaturases, lipases, and lipid transporters during and after metal exposure would give some hints about whether this is correct.

Another interesting observation would be the effect of BSO in lipid droplet formation levels. The unknown link between phytochelatin action and metal handling via lipid droplets requires further study to have a clearer picture of these mechanisms. Metabolic studies may be a useful tool to figure this out. Given the possible increase in electron density showed by lipid vesicles, we could hypothesise that phytochelatins like glutathione (GSH) bind to the lipid droplet's monolayer carrying lead with them to the vacuole for disposal.

In addition, it is not illogical to think that several metal handling mechanisms may operate simultaneously and still be correlated, establishing a metal handling system which optimises the response to stress. With this in mind, we considered a third metal handling mechanism to be involved: some organisms synthesise insoluble metal compounds, such as metal sulfides,

to stop these particles from harming the cells (Perales-Vela, Peña-Castro, & Cañizares-Villanueva, 2006; Bai & Zhang, 2009; Seshadri, Saranya, & Kowshik, 2011). Given *Ulva´*s high importance in marine sulfur cycles and its significant content of this element (De Clerck et al., 2018), lead sulfide (PbS) seems to be a good candidate to form insoluble lead aggregates.

Our new hypothesis considers these three mechanisms as part of a whole metal handling pathway. The model we propose for this mechanism is illustrated in Figure 22.

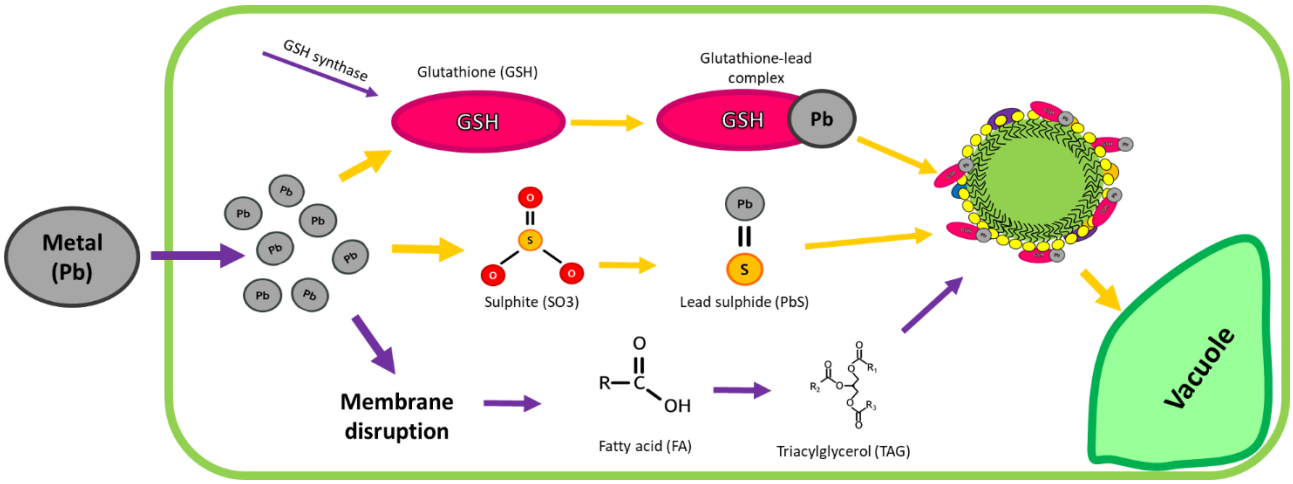

Figure 22 Proposed metal handling model for Ulva spp.
The yellow arrows follow those parts of the path for which we do not yet have any evidence. The purple arrows follow the path for which we currently have some evidence or indication.

This proposed model begins with metal triggering the three mechanisms at the same time. Oxidative stress would increase the amount of fatty acids which are pulled to TAG synthesis and lipid droplet formation. Simultaneously, lead would react with sulfite (SO_3) present in *Ulva* cells to form PbS which is later incorporated into the lipid droplet's surface as well as GSH-Pb complex, formed by glutathione and lead particles. There is evidence that lead and sulfur are present in a 1:2 proportion, there being twice as much sulfur than lead, suggesting that PbS might be sequestered by a metallothionein or a phytochelatin, like GSH (Seshadri, Saranya, & Kowshik, 2011). Also, the *Ulva* genome encodes the enzymes required for sulfite synthesis from hydrogen sulfide (H_2S), which have been identified in plants (Filipovic & Jovanović, 2017). Since all the compounds and enzymes required for these processes are present in *Ulva*, this model seems feasible.

5.5 X-Ray diffraction (XRD)

To test our new hypothesis, we needed to confirm the presence of PbS in our lead-treated cells. To do so, we chose X-Ray diffraction as the tool to use given our access to it and given that it is a common analysis for lead sulfide identification (Bai & Zhang, 2009; Kalita et al., 2012; Seshadri, Saranya, & Kowshik, 2011).

The XRD pattern obtained from analysing our lead-treated sample shows a significant increment in the diffraction intensity at 28.2°. Although this 2θ value may not seem significantly close to 29.96° it is possible that, given the 'amorphous' (not crystalline) structure of our sample, the X-rays may be diverted, modifying the diffraction angle to some extent. In addition, the culture media was not washed out before freeze-drying. Hence, we cannot be sure that the salts present in the artificial seawater are not interfering. Trials on control and lead culture media as well as a reading for PbS mixed with the control sample may shed some light on this and help to get clearer conclusions.

Because of the high likelihood of salt contamination, XRD patterns for Sodium (Na) compounds were also searched for to compare their 2θ values with our stronger signal (31.8°). As a result of that search, we found that Sodium salts, *e.g*. Sodium Chloride (NaCl) and Sodium Sulfate (Na_2SO_4), diffract X-rays between 31° and 32° 2θ values (Grass & Stark, 2005; Li, Chen, Zhou, Gu, & Chen, 2005; Linnow, Zeunert, & Steiger, 2006; Rasmussen, Jørgensen, & Lundtoft, 1996). Hence, we can conclude our highest peak corresponds to Sodium diffraction.

6 Conclusion

To conclude, finding alternative sources of energy that let us depend less and less on fossil fuels is crucial to avoid a highly likely energy crisis. This task may be partly fulfilled by biofuel implementation. To make renewable energy more popular and improve sustainable biofuel production, it is necessary to find the most suitable crop. In this work, we have shown that macroalgal lipids may be a promising candidate as a biodiesel feedstock for many reasons: lack of land competition, high growth rate and the potential implementation of phytoremediation systems in harvesting areas. *Ulva*'s capacity to grow under stress conditions makes it an interesting alternative feedstock. Such capacity has been indicated by the increased rates of lipid droplet formation and the recovery we observed after metal exposure.

However, this work has also demonstrated how little we know about algal metabolism and how necessary this knowledge is if we want to manipulate these pathways in order to increase *Ulva*'s neutral lipid availability. Factors like the lipid vesicles found during fluorescence imaging (c.f. § 4.2.1, Figure 12), the putative pyrenoids (c.f. § 4.2.1 Figure 8), as well as the XRD patterns we obtained suggest that metal handling happens through diverse mechanisms which remain unknown. Much deeper and broader studies have been carried out with microalgae as the object of study. However, even microalgal studies are in a very young stage. Given that the pathways known tend to be based in genomic predictions and not actual metabolism experiments, broader and deeper metabolic analyses are needed.

This project has tried to describe lipid droplet dynamics before, during and after metal exposure, as well as during the inhibition of parallel metal handling mechanisms. These trials have let us observe more closely and in higher detail how lipid droplets change in response to the presence of metal. Despite our answers, we also raised several questions for further study: much deeper observation of lipid droplets is necessary to get the complete picture. A closer look at these structures' dynamics as well as diffusion studies and comparisons in other kinds of stress would be of great benefit.

In addition, these experiments have made evident that metal handling mechanisms are not completely independent, and it is very likely they happen at the same time and they are

interdependent. Metabolomic studies, deeper genetic expression analysis and fatty acid characterisation could be important tools to retrieve the data needed to decipher the actual process. Metabolomic studies, for example, may help to determine the lipid source from which lipid droplets are formed. Also, it is essential to have more detailed knowledge of a broader range of lipid droplet proteins. This could be one key to establishing whether our metal handling model is a series of steps to form metal-carrying lipid droplets, or if they are independent processes.

Given the incredible amount of questions it is easy to forget this has the principal aim of testing the suitability of *Ulva* as a biofuel crop. However, it is essential to carry on forward research about *Ulva´*s metabolism and algal metabolism in general. Understanding algal metabolism to a greater extent will allow us to manipulate it and get bioproducts of interest in a more sustainable way. The final objective would be getting the ability of triggering lipid droplet formation without the necessity of an external agent.

In summary, this project has attempted to explain the changes in lipid metabolism as a consequence of heavy metal exposure. As a result, we propose a model that involves more mechanisms and processes than we expected. Although it seems feasible, our mechanism is speculative. Further studies and work orientated towards pathway elucidation are required to evaluate *Ulva* as a biofuel crop more objectively.

7 Appendix

7.1 A.1. Genes known to be related with lipid droplet formation in the *C. reinhardtii* genome.

Gene	Protein name	Source
CrIRE1	Inositol requiring enzyme	(Yamaoka et al., 2018)
CrLPAAT2	Chlorophyte specific Lysophosphatidic acid acyltransferase	(Kim, Terng, Riekhof, Cahoon, & Cerutti, 2018)
TOR	Target of rapamycin	(Pugkaew, Meetam, Ponpuak, Yokthongwattana, & Pokethitiyook, 2017)
DGAT1	Diacylglycerol acyltransferase	(Boyle et al., 2012)
DGTT1	Diacylglycerol O-acetyltransferase type 2	
PDAT1	Phospholipid:diacylglycerol acyltransferase	
MLDP	Major lipid droplet protein	(Moriyama, Toyoshima, Saito, Wada, & Sato, 2017)
CrACX2	Acyl-CoA oxidase	(Kong et al., 2017)
CrDGTT2	Diacylglycerol O-acetyltransferase type-2 2	(Zienkiewicz, Du, Ma, Vollheyde, & Benning, 2016)
GPAT	Glycerol-3-phosphate-acyltransferase	
LPAT	Lysophosphatidic acid acyltransferase	
CrPAP1	Phosphatidic acid phosphatase 1	
CrPAP2	Phosphatidic acid phosphatase 2	
CrDGTT2	Diacylglycerol acyltransferase type 2 2	
CrDGTT3	Diacylglycerol acyltransferase type 2 3	
NRR1	Nitrogen responsive regulator 1	
BTA1	DGTS Synthesis protein	(Goold et al., 2016)

CFA2	Cyclopropane-fatty acyl-phospholipid synthase	
GHL1	Glycosil hydrolase 1	
LCS2	Long chain Acyl-CoA synthetase	
TUB1	β tubulin	
LPLAT	Lysophospholipid acyltransferase	
α/β-Hydrolase	α/β-Hydrolase	
TGD2	Permease-like component of an ATP-binding cassette transporter	
CIS	Citrate synthase	(Goncalves, Wilkie, Kirst, & Rathinasabapathi, 2016)
LIP1	Lipase 1	
PGD1	Plastid galactoglycerolipid degradation 1	
TAR1	Triacylglycerol accumulation regulator 1	
ROC40	Rhythm of chloroplast 40	
TGD2	Trigalactosyldiacylglycerol 2	(Warakanont et al., 2015)
DGAT2	Diacylglycerol acyltransferase 2	(Manandhar-Shrestha & Hildebrand, 2015)
ACS2	Acetyl-CoA synthetase	(Ramanan et al., 2013)
GPAT	Glycerol-3-phosphate acyltransferase	(Nguyen et al., 2011)
LPAT	Lysophosphatidic acid acyltransferase	
Caleosin-like 1 and 2		(James et al., 2011)
Oleosin-like 1 and 2		

8 References

Abomohra, A., El-Naggar, A. and Baeshen, A. (2018). Potential of macroalgae for biodiesel production: Screening and evaluation studies. Journal of Bioscience and Bioengineering, 125(2), pp.231-237.

Adams, C., Godfrey, V., Wahlen, B., Seefeldt, L., & Bugbee, B. (2013). Understanding precision nitrogen stress to optimize the growth and lipid content tradeoff in oleaginous green microalgae. Bioresource Technology, 131, 188-194. doi: 10.1016/j.biortech.2012.12.143

Agarwal, A. (2007). Biofuels (alcohols and biodiesel) applications as fuels for internal combustion engines. Progress in Energy and Combustion Science, 33(3), pp.233-271.

Agunbiade, F., Olu-Owolabi, B. and Adebowale, K. (2009). Phytoremediation potential of Eichornia crassipes in metal-contaminated coastal water. Bioresource Technology, 100(19), pp.4521-4526.

Andrade, L. R., Farina, M., & Amado Filho, G. M. (2004). Effects of copper on Enteromorpha flexuosa (Chlorophyta) in vitro. Ecotoxicology and Environmental Safety, 58(1), 117–125. https://doi.org/10.1016/s0147-6513(03)00106-4

Atehortua, E. and Gartner, C. (2013). Estudios preliminares de la biomasa seca de eichhornia crassipes como adsorbente de plomo y cromo en aguas. Revista colombiana de materiales, (4), pp.81-92.

Bai, H.-J., & Zhang, Z.-M. (2009). Microbial synthesis of semiconductor lead sulfide nanoparticles using immobilized Rhodobacter sphaeroides. Materials Letters, 63(9–10), 764–766. https://doi.org/10.1016/j.matlet.2008.12.050

Baños, R., Manzano-Agugliaro, F., Montoya, F., Gil, C., Alcayde, A., & Gómez, J. (2011). Optimization methods applied to renewable and sustainable energy: A review. Renewable and Sustainable Energy Reviews, 15(4), 1753-1766. doi: 10.1016/j.rser.2010.12.008

Ben A. Silverberg (1975) Ultrastructural localization of lead in Stigeoclonium tenue (Chlorophyceae, Ulotrichales) as demonstrated by cytochemical and X-ray microanalysis, Phycologia, 14:4, 265-274, DOI: 10.2216/i0031-8884-14-4-265.1

Bolton, J., Cyrus, M., Brand, M., Joubert, M., & Macey, B. (2016). Why grow Ulva? Its potential role in the future of aquaculture. Perspectives in Phycology, 3(3), 113-120. doi: 10.1127/pip/2016/0058

BOSE, S. R. (1941). Function of Pyrenoids in Algæ. Nature, 148(3754), 440–441. https://doi.org/10.1038/148440a0

Boyle, N. R., Page, M. D., Liu, B., Blaby, I. K., Casero, D., Kropat, J., … Merchant, S. S. (2012a). Three Acyltransferases and Nitrogen-responsive Regulator Are Implicated in Nitrogen Starvation-induced Triacylglycerol Accumulation inChlamydomonas. Journal of Biological Chemistry, 287(19), 15811–15825. https://doi.org/10.1074/jbc.m111.334052

Cai, Y., McClinchie, E., Price, A., Nguyen, T., Gidda, S., Watt, S., Yurchenko, O., Park, S., Sturtevant, D., Mullen, R., Dyer, J. and Chapman, K. (2017). Mouse fat storage-inducing transmembrane protein 2 (FIT2) promotes lipid droplet accumulation in plants. Plant Biotechnology Journal, 15(7), pp.824-836.

Chávez-Sifontes, M., & Domine, M. (2013). LIGNIN, STRUCTURE AND APPLICATIONS: DEPOLYMERIZATION METHODS FOR OBTAINING AROMATIC DERIVATIVES OF INDUSTRIAL INTEREST. *Avances en Ciencias e Ingeniería, 4* (4), 15-46.

Chisti, Y. (2007). Biodiesel from microalgae. Biotechnology Advances, 25(3), 294-306. doi: 10.1016/j.biotechadv.2007.02.001

Davidi, L., Katz, A., & Pick, U. (2012). Characterization of major lipid droplet proteins from Dunaliella. Planta, 236(1), 19–33. https://doi.org/10.1007/s00425-011-1585-7

De Clerck, O., Kao, S., Bogaert, K., Blomme, J., Foflonker, F., & Kwantes, M. et al. (2018). Insights into the Evolution of Multicellularity from the Sea Lettuce Genome. Current Biology, 28(18), 2921-2933.e5. doi: 10.1016/j.cub.2018.08.015

Demirbas A. (2009a) Introduction. In: Biofuels. Green Energy and Technology. Springer, London.

Demirbas, A. (2009b). Biofuels securing the planet's future energy needs. *Energy Conversion and Management*, *50*(9), 2239-2249. doi: 10.1016/j.enconman.2009.05.010

Demirbas, A. (2009c) Biomass Feedstocks. In: Biofuels. Green Energy and Technology. Springer, London

Demirbas. (2009d) Biofuels. In: Biofuels. Green Energy and Technology. Springer, London.

Deng, X., Cai, J., & Fei, X. (2013). Effect of the expression and knockdown of citrate synthase gene on carbon flux during triacylglycerol biosynthesis by green algae Chlamydomonas reinhardtii. BMC Biochemistry, 14(1), 38. https://doi.org/10.1186/1471-2091-14-38

El Maghraby, D. and Fakhry, E. (2015). Lipid content and fatty acid composition of Mediterranean macro-algae as dynamic factors for biodiesel production. Oceanologia, 57(1), pp.86-92.

Emamverdian, A., Ding, Y., Mokhberdoran, F. and Xie, Y. (2015). Heavy Metal Stress and Some Mechanisms of Plant Defense Response. The Scientific World Journal, 2015, pp.1-18.

EPA (United States Environmental Protection Agency, Air and Radiation). (2002). *A comprehensive analysis of biodiesel impacts on exhaust emissions*. Retrieved from https://nepis.epa.gov/Exe/ZyPURL.cgi?Dockey=P1001ZA0.txt

Fujimoto, T., & Parton, R. G. (2011). Not Just Fat: The Structure and Function of the Lipid Droplet. Cold Spring Harbor Perspectives in Biology, 3(3), a004838–a004838. https://doi.org/10.1101/cshperspect.a004838

Ge, C., Yu, X., Kan, M., & Qu, C. (2017). Adaption of Ulva pertusa to multiple contamination of heavy metals and nutrients: Biological mechanism of outbreak of Ulva sp. green tide. Marine Pollution Bulletin, 125(1-2), 250-253. doi: 10.1016/j.marpolbul.2017.08.025

Gibbs, S. P. (1962). The ultrastructure of the pyrenoids of algae, exclusive of the green algae. Journal of Ultrastructure Research, 7(3–4), 247–261. https://doi.org/10.1016/s0022-5320(62)90021-7

Goh, C., & Lee, K. (2010). A visionary and conceptual macroalgae-based third-generation bioethanol (TGB) biorefinery in Sabah, Malaysia as an underlay for renewable and sustainable development. Renewable And Sustainable Energy Reviews, 14(2), 842-848. doi: 10.1016/j.rser.2009.10.001

Goncalves, E. C., Wilkie, A. C., Kirst, M., & Rathinasabapathi, B. (2016). Metabolic regulation of triacylglycerol accumulation in the green algae: identification of potential targets for engineering to improve oil yield. Plant Biotechnology Journal, 14(8), 1649–1660. https://doi.org/10.1111/pbi.12523

Goold, H. D., Cuiné, S., Legeret, B., Liang, Y., Brugière, S., Auroy, P., … Li-Beisson, Y. (2016). Saturating Light Induces Sustained Accumulation of Oil in Plastidal Lipid Droplets in Chlamydomonas reinhardtii. Plant Physiology, 171, pp.00718.2016. https://doi.org/10.1104/pp.16.00718

Gosch, B., Magnusson, M., Paul, N. and de Nys, R. (2012). Total lipid and fatty acid composition of seaweeds for the selection of species for oil-based biofuel and bioproducts. GCB Bioenergy, 4(6), pp.919-930.

Grass, R. N., & Stark, W. J. (2005). Flame synthesis of calcium-, strontium-, barium fluoride nanoparticles and sodium chloride. Chemical Communications, (13), 1767. https://doi.org/10.1039/b419099h

Griffith OW, Meister A (1979) Potent and specific inhibition of glutathione synthesis by buthionine sulfoximine (S-n-butyl homocysteine sulfoximine). J Biol Chem 254:7558–7560.

Guo, Y., Cordes, K., Farese, R. and Walther, T. (2009). Lipid droplets at a glance. Journal of Cell Science, 122(6), pp.749-752.

Harrison, P.J., R.E. Waters and F.J.R. Taylor. 1980. A broad spectrum artificial medium for coastal and open ocean phytoplankton. J. Phycol. 16:28-35.

Hashemi, H. F., & Goodman, J. M. (2015). The life cycle of lipid droplets. Current Opinion in Cell Biology, 33, 119–124. https://doi.org/10.1016/j.ceb.2015.02.002

Hossain, M. A., Piyatida, P., da Silva, J. A. T., & Fujita, M. (2012). Molecular Mechanism of Heavy Metal Toxicity and Tolerance in Plants: Central Role of Glutathione in Detoxification of Reactive Oxygen Species and Methylglyoxal and in Heavy Metal Chelation. Journal of Botany, 2012, 1–37. https://doi.org/10.1155/2012/872875

IPCC, 2014: Summary for Policymakers. In: Climate Change 2014: Mitigation of Climate Change. Contribution of Working Group III to the Fifth Assessment Report of the Intergovernmental Panel on Climate Change [Edenhofer, O., R. Pichs-Madruga, Y. Sokona, E. Farahani, S. Kadner, K. Seyboth, A. Adler, I. Baum, S. Brunner, P. Eickemeier, B. Kriemann, J. Savolainen, S. Schlömer, C. von Stechow, T. Zwickel and J.C. Minx (eds.)]. Cambridge University Press, Cambridge, United Kingdom and New York, NY, USA.

Iwai, M., Ikeda, K., Shimojima, M., & Ohta, H. (2014). Enhancement of extraplastidic oil synthesis inChlamydomonas reinhardtiiusing a type-2 diacylglycerol acyltransferase with a phosphorus starvation-inducible promoter. Plant Biotechnology Journal, 12(6), 808-819. doi: 10.1111/pbi.12210

James, G. O., Hocart, C. H., Hillier, W., Chen, H., Kordbacheh, F., Price, G. D., & Djordjevic, M. A. (2011). Fatty acid profiling of Chlamydomonas reinhardtii under nitrogen deprivation. Bioresource Technology, 102(3), 3343–3351. https://doi.org/10.1016/j.biortech.2010.11.051

John, R., Anisha, G., Nampoothiri, K. and Pandey, A. (2011). Micro and macroalgal biomass: A renewable source for bioethanol. Bioresource Technology, 102(1), pp.186-193.

Kalita, M. P. C., Deka, K., Das, J., Hazarika, N., Dey, P., Das, R., … Sarma, B. K. (2012). X-ray diffraction line profile analysis of chemically synthesized lead sulphide nanocrystals. Materials Letters, 87, 84–86. https://doi.org/10.1016/j.matlet.2012.07.098

Kim, B., Ramanan, R., Kang, Z., Cho, D., Oh, H., & Kim, H. (2016). Chlorella sorokiniana HS1, a novel freshwater green algal strain, grows and hyperaccumulates lipid droplets in seawater salinity. Biomass and Bioenergy, 85, 300-305. doi: 10.1016/j.biombioe.2015.12.026

Kim, Y., Terng, E. L., Riekhof, W. R., Cahoon, E. B., & Cerutti, H. (2018). Endoplasmic reticulum acyltransferase with prokaryotic substrate preference contributes to triacylglycerol assembly in Chlamydomonas. Proceedings of the National Academy of Sciences, 115(7), 1652–1657. https://doi.org/10.1073/pnas.1715922115

Kodama, Y. (2016). Time Gating of Chloroplast Autofluorescence Allows Clearer Fluorescence Imaging In Planta. PLOS ONE, 11(3), e0152484. https://doi.org/10.1371/journal.pone.0152484

Kong, F., Liang, Y., Légeret, B., Beyly-Adriano, A., Blangy, S., Haslam, R. P., … Li-Beisson, Y. (2017). Chlamydomonascarries out fatty acid β-oxidation in ancestral peroxisomes using a bona fide acyl-CoA oxidase. The Plant Journal, 90(2), 358–371. https://doi.org/10.1111/tpj.13498

Kumari, P., Kumar, M., Reddy, C., & Jha, B. (2013). Nitrate and Phosphate Regimes Induced Lipidomic and Biochemical Changes in the Intertidal Macroalga Ulva lactuca (Ulvophyceae, Chlorophyta). Plant and Cell Physiology, 55(1), 52-63. doi: 10.1093/pcp/pct156

Li, Y. X., Chen, W. F., Zhou, X. Z., Gu, Z. Y., & Chen, C. M. (2005). Synthesis of CeO2 nanoparticles by mechanochemical processing and the inhibiting action of NaCl on particle agglomeration. Materials Letters, 59(1), 48–52. https://doi.org/10.1016/j.matlet.2004.05.089

Li-Beisson, Y. (2018). Triacylglycerol Biosynthesis in Eukaryotic Microalgae - AOCS Lipid Library. [online] Lipidlibrary.aocs.org. Available at: http://lipidlibrary.aocs.org/Biochemistry/content.cfm?ItemNumber=40313 [Accessed 24 Apr. 2018].

Linnow, K., Zeunert, A., & Steiger, M. (2006). Investigation of Sodium Sulfate Phase Transitions in a Porous Material Using Humidity- and Temperature-Controlled X-ray Diffraction. Analytical Chemistry, 78(13), 4683–4689. https://doi.org/10.1021/ac0603936

Liu, B., & Benning, C. (2013). Lipid metabolism in microalgae distinguishes itself. Current Opinion in Biotechnology, 24(2), 300–309. https://doi.org/10.1016/j.copbio.2012.08.008

Liu, Z., Wang, G. & Zhou, B. (2008). Effect of iron on growth and lipid accumulation in Chlorella vulgaris. Bioresource Technology. Volume 99, Issue 11. Pages 4717-4722. https://doi.org/10.1016/j.biortech.2007.09.073.(http://www.sciencedirect.com/science/article/pii/S0960852407008292)

Lund, H. (2007). Renewable energy strategies for sustainable development. Energy, 32(6), 912-919. doi: 10.1016/j.energy.2006.10.017

Maceiras, R., Rodríguez, M., Cancela, A., Urréjola, S., & Sánchez, A. (2011). Macroalgae: Raw material for biodiesel production. Applied Energy, 88(10), 3318-3323. doi: 10.1016/j.apenergy.2010.11.027

Manandhar-Shrestha, K., & Hildebrand, M. (2015). Characterization and manipulation of a DGAT2 from the diatom Thalassiosira pseudonana: Improved TAG accumulation without detriment to growth, and implications for chloroplast TAG accumulation. Algal Research, 12, 239–248. https://doi.org/10.1016/j.algal.2015.09.004

Mathur, S., Agrawal, D. and Jajoo, A. (2014). Photosynthesis: Response to high temperature stress. Journal of Photochemistry and Photobiology B: Biology, 137, pp.116-126.

Mellado, M., Contreras, R., González, A., Dennett, G., & Moenne, A. (2012). Copper-induced synthesis of ascorbate, glutathione and phytochelatins in the marine alga Ulva compressa (Chlorophyta). Plant Physiology and Biochemistry, 51, 102-108. doi: 10.1016/j.plaphy.2011.10.007

Michalak, I. (2018). Experimental processing of seaweeds for biofuels. Wiley Interdisciplinary Reviews: Energy and Environment, 7(3), p. e288.

Moenne, A., González, A., & Sáez, C. A. (2016). Mechanisms of metal tolerance in marine macroalgae, with emphasis on copper tolerance in Chlorophyta and Rhodophyta. Aquatic Toxicology, 176, 30–37. https://doi.org/10.1016/j.aquatox.2016.04.015

Mohy El-Din, S. (2017). Fatty acid profiling as bioindicator of chemical stress in marine Pterocladia capillacea, Sargassum hornschuchii and Ulva lactuca. International Journal of Environmental Science and Technology, 15(4), pp.791-800.

Moomaw, W., F. Yamba, M. Kamimoto, L. Maurice, J. Nyboer, K. Urama, T. Weir, 2011: Introduction. In IPCC Special Report on Renewable Energy Sources and Climate Change Mitigation [O. Edenhofer, R. Pichs-Madruga, Y. Sokona, K. Seyboth, P. Matschoss, S. Kadner, T. Zwickel, P. Eickemeier, G. Hansen, S. Schlömer, C.von Stechow (eds)], Cambridge University Press, Cambridge, United Kingdom and New York, NY, USA.

Moriyama, T., Toyoshima, M., Saito, M., Wada, H., & Sato, N. (2017). Revisiting the Algal "Chloroplast Lipid Droplet": The Absence of an Entity That Is Unlikely to Exist. Plant Physiology, 176(2), 1519–1530. https://doi.org/10.1104/pp.17.01512

Naik, S., Goud, V., Rout, P., & Dalai, A. (2010). Production of first- and second-generation biofuels: A comprehensive review. Renewable and Sustainable Energy Reviews, 14(2), 578-597. doi: 10.1016/j.rser.2009.10.003

Nas, B., & Berktay, A. (2007). Energy Potential of Biodiesel Generated from Waste Cooking Oil: An Environmental Approach. *Energy Sources, Part B: Economics, Planning, And Policy*, *2*(1), 63-71. doi: 10.1080/15567240500400903

Nguyen, H. M., Baudet, M., Cuiné, S., Adriano, J.-M., Barthe, D., Billon, E., … Li-Beisson, Y. (2011). Proteomic profiling of oil bodies isolated from the unicellular green microalga Chlamydomonas reinhardtii: With focus on proteins involved in lipid metabolism. PROTEOMICS, 11(21), 4266–4273. https://doi.org/10.1002/pmic.201100114

Ohsaki, Y., Shinohara, Y., Suzuki, M., & Fujimoto, T. (2010). A pitfall in using BODIPY dyes to label lipid droplets for fluorescence microscopy. Histochemistry and Cell Biology, 133(4), 477–480. https://doi.org/10.1007/s00418-010-0678-x

Perales-Vela, H. V., Peña-Castro, J. M., & Cañizares-Villanueva, R. O. (2006). Heavy metal detoxification in eukaryotic microalgae. Chemosphere, 64(1), 1–10. https://doi.org/10.1016/j.chemosphere.2005.11.024

Pugkaew, W., Meetam, M., Ponpuak, M., Yokthongwattana, K., & Pokethitiyook, P. (2017). Role of autophagy in triacylglycerol biosynthesis in Chlamydomonas reinhardtii revealed by chemical inducer and inhibitors. Journal of Applied Phycology, 30(1), 15–22. https://doi.org/10.1007/s10811-017-1166-7

Pyc, M., Cai, Y., Greer, M., Yurchenko, O., Chapman, K., Dyer, J. and Mullen, R. (2017). Turning Over a New Leaf in Lipid Droplet Biology. Trends in Plant Science, 22(7), pp.596-609.

Ramanan, R., Kim, B.-H., Cho, D.-H., Ko, S.-R., Oh, H.-M., & Kim, H.-S. (2013). Lipid droplet synthesis is limited by acetate availability in starchless mutant of Chlamydomonas reinhardtii. FEBS Letters, 587(4), 370–377. https://doi.org/10.1016/j.febslet.2012.12.020

Rasmussen, S. E., Jørgensen, J. E., & Lundtoft, B. (1996). Structures and Phase Transitions of Na2SO4. Journal of Applied Crystallography, 29(1), 42–47. https://doi.org/10.1107/s0021889895008818

Ruan, Y., Jin, Y., Yang, Y., Li, G. and Boyer, J. (2010). Sugar Input, Metabolism, and Signaling Mediated by Invertase: Roles in Development, Yield Potential, and Response to Drought and Heat. Molecular Plant, 3(6), pp.942-955.

Rueden, C. T.; Schindelin, J. & Hiner, M. C. et al. (2017), "ImageJ2: ImageJ for the next generation of scientific image data", BMC Bioinformatics 18:529, doi:10.1186/s12859-017-1934-z.

S. R. Bose, "Role of Pyrenoids in Algae and of Vacuoles in Plastids of Higher and in Fungi," Botanical Gazette 104, no. 4 (Jun., 1943): 633-638.

Saga, K., Yokoyama, S., Imou, K., & Kaizu, Y. (2008). A Comparative Study of the Effect of CO2 Emission Reduction by Several Bioenergy Production Systems. International Energy Journal, 9(Special issue), 53-60.

Salama, E., Kim, H., Abou-Shanab, R., Ji, M., Oh, Y., Kim, S., & Jeon, B. (2013). Biomass, lipid content, and fatty acid composition of freshwater Chlamydomonas mexicana and Scenedesmus obliquus grown under salt stress. Bioprocess And Biosystems Engineering, 36(6), 827-833. doi: 10.1007/s00449-013-0919-1

Sánchez, C. (2009). Lignocellulosic residues: Biodegradation and bioconversion by fungi. *Biotechnology Advances*, *27*(2), 185-194. doi: 10.1016/j.biotechadv.2008.11.001

Schindelin, J., Arganda-Carreras, I., Frise, E., Kaynig, V., Longair, M., & Pietzsch, T. et al. (2012). Fiji: an open-source platform for biological-image analysis. Nature Methods, 9(7), 676-682. doi: 10.1038/nmeth.2019

Scott, D. W. (2015). *Multivariate density estimation : theory, practice, and visualization*. Hoboken Nj: Wiley.

Seshadri, S., Saranya, K., & Kowshik, M. (2011). Green synthesis of lead sulfide nanoparticles by the lead resistant marine yeast, Rhodosporidium diobovatum. Biotechnology Progress, 27(5), 1464–1469. https://doi.org/10.1002/btpr.651

Sheehan, J., Camobreco, V., Duffield, J., Shapouri, H., Graboski, M., & Tyson, K. S. An Overview of Biodiesel and Petroleum Diesel Life Cycles. United States. doi:10.2172/771560.

Suutari, M., Leskinen, E., Fagerstedt, K., Kuparinen, J., Kuuppo, P. and Blomster, J. (2014). Macroalgae in biofuel production. Phycological Research, 63(1), pp.1-18.

Suzuki M., Shinohara Y., Fujimoto T. (2012) Histochemical Detection of Lipid Droplets in Cultured Cells. In: Taatjes D., Roth J. (eds) Cell Imaging Techniques. Methods in Molecular Biology (Methods and Protocols), vol 931. Humana Press, Totowa, NJ

Teng, L., Ding, L., & Lu, Q. (2011). Microscopic observation of pyrenoids in Order Ulvales (Chlorophyta) collected from Qingdao coast. Journal of Ocean University of China, 10(3), 223–228. https://doi.org/10.1007/s11802-011-1777-6

Thakur, P., Kumar, S., Malik, J. A., Berger, J. D., & Nayyar, H. (2010). Cold stress effects on reproductive development in grain crops: An overview. Environmental and Experimental Botany, 67(3), 429–443. https://doi.org/10.1016/j.envexpbot.2009.09.004

Upchurch, R. (2008). Fatty acid unsaturation, mobilization, and regulation in the response of plants to stress. Biotechnology Letters, 30(6), 967-977. doi: 10.1007/s10529-008-9639-z

Vicente, G., Martínez, M., & Aracil, J. (2004). Integrated biodiesel production: a comparison of different homogeneous catalysts systems. Bioresource Technology, 92(3), 297-305. doi: 10.1016/j.biortech.2003.08.014

Wang, Z.T., Ullrich, N., Joo, S., Waffenschmidt, S. & Goodenough, U., (2009). Algal Lipid Bodies: Stress Induction, Purification, and Biochemical Characterization in Wild-Type and Starchless Chlamydomonas reinhardtii. Eukaryotic Cell, 8 (12) 1856-1868; DOI: 10.1128/EC.00272-09

Warakanont, J., Tsai, C.-H., Michel, E. J. S., Murphy, G. R., Hsueh, P. Y., Roston, R. L., … Benning, C. (2015). Chloroplast lipid transfer processes in Chlamydomonas reinhardtii involving a

TRIGALACTOSYLDIACYLGLYCEROL 2 (TGD2) orthologue. The Plant Journal, 84(5), 1005–1020. https://doi.org/10.1111/tpj.13060

Wei, N., Quarterman, J. and Jin, Y. (2013). Marine macroalgae: an untapped resource for producing fuels and chemicals. Trends in Biotechnology, 31(2), pp.70-77.

Welte, M. (2015). Expanding Roles for Lipid Droplets. Current Biology,Volume 25, Issue 11. Pages R470-R481. https://doi.org/10.1016/j.cub.2015.04.004(http://www.sciencedirect.com/science/article/pii/S0960982215004170)

Yamaoka, Y., Choi, B. Y., Kim, H., Shin, S., Kim, Y., Jang, S., … Lee, Y. (2018). Identification and functional study of the endoplasmic reticulum stress sensor IRE1 in Chlamydomonas reinhardtii. The Plant Journal, 94(1), 91–104. https://doi.org/10.1111/tpj.13844

Zienkiewicz, K., Du, Z.-Y., Ma, W., Vollheyde, K., & Benning, C. (2016). Stress-induced neutral lipid biosynthesis in microalgae — Molecular, cellular and physiological insights. Biochimica et Biophysica Acta (BBA) - Molecular and Cell Biology of Lipids, 1861(9), 1269–1281. https://doi.org/10.1016/j.bbalip.2016.02.008